

Washington University in St. Louis

Washington University Open Scholarship

Engineering and Applied Science Theses &
Dissertations

McKelvey School of Engineering

Spring 2021

An Injectable Thermosensitive Hydrogel Potentially Used for Wound Dressing with Self-adhesive Properties

Yunxiu Qiu

Washington University in St. Louis

Follow this and additional works at: https://openscholarship.wustl.edu/eng_etds



Part of the [Biology and Biomimetic Materials Commons](#)

Recommended Citation

Qiu, Yunxiu, "An Injectable Thermosensitive Hydrogel Potentially Used for Wound Dressing with Self-adhesive Properties" (2021). *Engineering and Applied Science Theses & Dissertations*. 568.
https://openscholarship.wustl.edu/eng_etds/568

This Thesis is brought to you for free and open access by the McKelvey School of Engineering at Washington University Open Scholarship. It has been accepted for inclusion in Engineering and Applied Science Theses & Dissertations by an authorized administrator of Washington University Open Scholarship. For more information, please contact digital@wumail.wustl.edu.

Washington University in St. Louis
McKelvey School of Engineering
Department of Mechanical Engineering and Material Science

Thesis Examination Committee:

Jianjun Guan

Spencer Lake

Srikanth Singamaneni

An Injectable Thermosensitive Hydrogel
Potentially Used for Wound Dressing with Self-adhesive Properties

By

Yunxiu Qiu

A thesis presented to
the McKelvey School of Engineering of Washington University in St. Louis
in partial fulfillment of the requirements for the degree of Master of Science

May 2021

St. Louis, Missouri

© 2021 Yunxiu Qiu

Table of Contents

List of Tables	iii
List of Figures	iv
List of Acronym and Abbreviations	vi
Acknowledgements	viii
Abstract	ix
Chapter 1: Introduction	1
1.1 Injectable hydrogels used in wound dressing	1
1.2 Thermosensitive hydrogels used in would dressing	2
1.2.1 PNIPAM-based hydrogels	2
1.2.2 Dopamine-modified hydrogels in wound dressing	3
1.3 Functional domains used in hydrogels.....	3
1.4 Mesenchymal stem cells used in wound dressing.....	4
1.5 Silver Nano-Coatings used as antibacterial potential for wound dressing	5
Chapter 2: An Injectable Thermosensitive Hydrogel Potentially Used for Wound Dressing with Self-adhesive Properties.....	6
2.1 Material and methods.....	6
2.1.1 Materials	6
2.1.2 Synthesis of Polymer I.....	7
2.1.3 Conjugation of Polymer II	8
2.1.4 Characterization of synthesized hydrogel	9
2.1.5 Solubility, injectability and thermosensitive gelation	9
2.1.6 Water content of synthesized hydrogel.....	9

2.1.7	In vitro degradation.....	10
2.1.8	Rheology test	11
2.1.9	Lap shear adhesion test.....	11
2.1.10	Cell culture.....	12
2.1.11	Cytotoxicity of degradation media.....	14
2.1.12	Cell growth on synthesized hydrogels	15
2.1.13	Cell adhesion and morphology on hydrogels.....	16
2.1.14	Animal experiment.....	17
2.2	Results and Discussions.....	18
2.2.1	Synthesis and characterizations of hydrogels	18
2.2.2	Solubility, injectability and thermosensitive gelation.....	19
2.2.3	In vitro degradation and water content	20
2.2.4	Rheology test	21
2.2.5	Lap shear adhesion tests and tissue adhesion	22
2.2.6	Cytotoxicity of degradation media.....	23
2.2.7	Cell growth on hydrogels.....	23
2.2.8	Cell adhesion and morphology on hydrogels.....	25
2.2.9	In vivo biocompatibility.....	26
2.3	Conclusions.....	27
Chapter 3:	Future work	28
3.1	Further improvements of hydrogel properties	28
3.2	Antibacterial Ag-coated dopamine hydrogel	28
References	47

List of Tables

Table 1 <i>Feed ratio and real ratio of synthesized Polymer I and Polymer II.</i>	42
Table 2 <i>Degradation remaining weight of synthesized hydrogels.</i>	43
Table 3 <i>Water content of synthesized hydrogels.</i>	43
Table 4 <i>LCST of synthesized hydrogels.</i>	44
Table 5 <i>Lap shear strength of D1/4 and D1/2 hydrogels.</i>	44
Table 6 <i>Cell viability percentage of MTT assay of RCFs growing on synthesized hydrogels.</i>	45
Table 7 <i>Light absorbance of reaction product of D1/4 and D1/2 hydrogels with MTT solution.</i>	45
Table 8 <i>Light absorbance of RMSCs MTT assay with dopamine-MTT solution reaction influence removed.</i>	45
Table 9 <i>Proportion of fluorescence absorbance of cell growth on synthesized hydrogels</i>	46

List of Figures

Figure 1. Synthesis of Polymer I.....	29
Figure 2. Conjugation of Polymer II. $x=0.25, 0.5$	29
Figure 3. ^1H NMR spectrum of synthesized polymer. (a) Polymer II, D1/2 hydrogel; (b) Polymer II, D1/4 hydrogel; (c) Polymer I, D0 hydrogel.	30
Figure 4. Solubility of synthesized polymers. (a) D0 hydrogel, (b) D1/4 hydrogel, and (c) D1/2 hydrogel. All dissolved at 4°C and gelled at 37°C	31
Figure 5. Injectability of synthesized polymers through 27 Gauge needles, at 4°C . (a) D0 hydrogel, (b) D1/4 hydrogel, and (c) D1/2 hydrogel.	31
Figure 6. Schematic illustration of degradation product of Polymer II.	32
Figure 7. Degradation of D1/4 and D1/2 hydrogels.	32
Figure 8. (a) Schematic illustration of lap shear adhesion tests. (b) Instron used to test the lap shear strength. (c) Direct adhesion between hydrogel and glass slides.	33
Figure 9. Adhesion between hydrogels and tissues. (a) D1/4 hydrogel with mouse kidney, (b) D1/4 hydrogel with mouse spleen, (c) D1/4 hydrogel with mouse liver; (d) D1/2 hydrogel with mouse heart, (e) D1/2 hydrogel with mouse kidney.	34
Figure 10. Cytotoxicity of degradation medium. Cell viability of day 7, 14, 21, 28 degradation media. $n=8$, ns: $p \geq 0.05$	35
Figure 11. Reaction between hydrogels and MTT solution. Absorbance spectrum of reaction product at 560 and 670 nm. $n=8$	36
Figure 12. MTT assay of RMSCs growth on synthesized hydrogels. Absorbance spectrum of MTT assay at 560 and 670 nm, influence of dopamine-MTT solution reaction is removed. $n=8$	36

Figure 13. Cell growth on synthesized hydrogels. dsDNA test of RMSCs growing on no treatment coverslip, D0 and D1/2 hydrogels after 1 and 2 days. n=4, *: p<0.05, **: p<0.01.....	37
Figure 14. Image of cell adhesion on hydrogels. (a)-(c) Confocal imaging of RMSCs grew on D0, D1/4 and D1/2 hydrogels after 6 hours; (d)-(f) RMSCs grew on D0, D1/4 and D1/2 hydrogels after 24 hours. Scale bar: 50µm.	38
Figure 15. 10× imaging of H&E staining after 5 days of subcutaneous injection skin slices. (a) Control group injected with collagen gel, (b) injected with D0 hydrogel, (c) injected with D1/4 hydrogel, and (d) D1/2 hydrogel. Scale bar: 100µm	39
Figure 16. H&E staining of subcutaneous injection samples, control group injected with collagen hydrogel. (a) 10× and (b) 20× magnificence imaging of slices.	40
Figure 17. H&E staining of subcutaneous injection samples, 200µL Polymer I solution (D0 hydrogel) injected. (a) 10× and (b) 20× magnificence imaging of slices.	40
Figure 18. H&E staining of subcutaneous injection samples, Polymer II solution (D1/4 hydrogel) injected with collagen hydrogel. (a) 10× and (b) 20× magnificence imaging of slices.....	41
Figure 19. H&E staining of subcutaneous injection samples, Polymer II solution (D1/2 hydrogel) injected with collagen hydrogel. (a) 10× and (b) 20× magnificence imaging of slices.....	41

List of Acronym and Abbreviations

Acronym and abbreviation	Full name
NIPAM	N-Isopropylacrylamide
PNIPAM	Poly (N-Isopropylacrylamide)
PEGMA	Poly (ethylene glycol) methacrylate
AOLA	Acrylate-oligolactide
NAS	N-acryloxysuccinimide
DOPA	Dopamine hydrochloride
Polymer I /D0 hydrogel	Poly (NIPAM-PEGMA-AOLA-NAS)
Polymer II	Poly (NIPAM-PEGMA-AOLA-NAS-DOPA _x)
D1/4 hydrogel	Polymer II, x=0.25
D1/2 hydrogel	Polymer II, x=0.5
NHS	N-hydroxysuccinimide
BPO	Benzoyl peroxide
AgNO ₃	Silver nitrate
Na ₂ CO ₃	Sodium carbonate

Na ₂ SO ₄	Sodium sulfate
Ac	Acryloyl-chloride
THF	Tetrahydrofuran
DMF	Dimethylformamide
TEA	Triethylamine
CHCl ₃	Chloroform
DCM	Dichloromethane
DI H ₂ O	Deionized water
PBS	Phosphate-buffered saline
DMEM	Dulbecco's modification of eagle's medium
MEM	Minimum essential medium
FBS	fetal bovine serum
Trypsin	Trypsin serine protease enzyme
Pen Strep	Penicillin streptomycin

Acknowledgements

Throughout the writing of this thesis, I have received a great deal of support and assistance.

First and foremost, I am extremely grateful to my research supervisor, Dr. Jianjun Guan.

Without his introduction and suggestion, I could not have the precious opportunity to join the lab and do the project. His insightful feedback pushed me to sharpen my thinking and brought my work to a higher level. I would like to specially thank Dr. Hong Niu for her valuable guidance throughout my studies. Her meticulous guidance helped me with my experiments and data analysis.

I would also like to thank all the previous and current members in Guan's lab, Dr. Ting Zhong, Yu Dang, Ya Guan, Ning Gao, Jiaying Wen, Zhongting Liu, Tianhong Zhou, Yubin Ying and Jin Zhai. It was their kind help and support that have made my study and life in the WashU a wonderful time. Also, I want to thank Ms. Barbara Semar for instrument guidance and Ms Crystal Idleburg for sectioning and staining skin slices for me.

In addition, I would like to express my gratitude to my mother Liqing Wang, my farther Nansheng Qiu, my friends Xiaohong Tan, Huanzhu Jiang and Yuze Xia. Without their tremendous understanding and encouragement in the past two years, it would be impossible for me to complete my study.

Yunxiu Qiu

May 2021

Abstract

An Injectable Thermosensitive Hydrogel
Potentially Used for Wound Dressing with Self-adhesive Properties

By

Yunxiu Qiu

Master of Science in Material Science and Engineering

Washington University in St. Louis, 2021

Research Advisor: Professor Jianjun Guan

Wound healing is a complex process, and different kinds of materials are tried to achieve rapid healing. Among them, hydrogel is one of the best candidates for wound dressing due to its distinctive properties, such as high biocompatibility, flexibility, and sensitivity to physiological environments. Injectable hydrogels can be easily delivered in vivo without massive impairment to the body, as no surgical incision is needed for hydrogel embedment. This is highly consistent with the need of minimal invasion on human body. Multiple stimuli could be applied to achieve its injectability, including pH, temperature, light, ions in body fluids. Thermosensitive hydrogel is commonly used due to its high retention of cells and drugs in the local sites. Poly (N-Isopropylacrylamide) (PNIPAM) could be applied because PNIPAM-based polymers can achieve fast gelling at body temperature. Additionally, the introduction of dopamine could provide self-adhesive property for wound dressing applications because of possible bonds with cells, tissues and inorganics. In this thesis, a series of PNIPAM-based, dopamine-modified hydrogels are prepared. They show rapid gelation, high water content, degradability, no

cytotoxicity of degradation product to cells, and high in vivo biocompatibility. These hydrogels could also improve cell adhesion as well as promoting cell growth and proliferation. Moreover, the hydrogels could potentially present anti-bacterial properties when silver could be coated onto the hydrogel, which could provide further advantages in wound dressing.

Chapter 1: Introduction

1.1 Injectable hydrogels used in wound dressing

Wound healing is a complex and dynamic process which is related with cell growth and tissue regeneration^[1]. To achieve a rapid wound closure rate, an environment with appropriate moisture is always required as well as microbial infection prevention^[2]. In previous works, several materials have been developed as wound dressing materials, such as hydrogels, hydrocolloids, synthetic foam dressings, silicone meshes, moisture-permeable adhesive films, and silver/collagen-containing dressing^[3,4]. Among them, hydrogels outstands due to their biomimetic properties including high biocompatibility, proper stiffness and flexibility, sensitivity to physiological environments, and the ability to deliver drugs or growth factors to promote cell proliferation and tissue maturation^[5-7]. At the same time, hydrogel dressed at wound cite also allows oxygen to penetrate, absorbs exudate from wound cite as well as remaining moist environment as required^[8].

However, normal dressing hydrogels, which are usually sheet-like, have limits of fitting different shaped wounds. Therefore, injectable hydrogels have been noticed and applied on wound dressing^[9]. They can more easily fill wound cite and adhere to tissues^[10,11]. These self-healing hydrogels are injected into the body in liquid form and are instantly converted into solid hydrogels in situ by physical or chemical cross-linking. Stem cells, drugs, proteins or other biomolecules can be mixed with the precursor polymer solution before injection and then retained by the hydrogel network^[12]. In addition, injectable hydrogels can also achieve minimal invasion^[13]. To attain in situ gelling, several stimuli could be applied including pH, temperature, light, and ions in body fluids^[14-16].

1.2 Thermosensitive hydrogels used in wound dressing

1.2.1 PNIPAM-based hydrogels

Among all the stimuli that could form in situ injectable hydrogels, temperature is the most widely used as no other condition is needed as injected in vivo. Poly(N-Isopropylacrylamide) (PNIPAM)-based hydrogel is one of the most widely studied owing to its thermo-sensitivity, biocompatibility and great structure tailorability and flexibility^[17,18]. In an aqueous solution, as the temperature rises above the lower critical solution temperature (LCST) of approximately 32°C, PNIPAM undergoes a phase change from a hydrophilic state to a hydrophobic state^[19], ^[20].

However, PNIPAM-based hydrogels still have some limits on wound dressing due to few available functional groups. For instance, during the volume shrinkage of the hydrogel, stable adhesion between the hydrogel and the skin is also required to keep the hydrogel attached to the skin, so as to ensure that the contractile force of the hydrogel can help the wound to close^[19]. Several studies have been conducted to improve properties of PNIPAM-based hydrogels. For instance, collagen and hyaluronic acid were used to modify their biocompatibility, poly (amidoamine) (PAA) could also be added as crosslinker to improve stiffness^[21,22].

1.2.2 Dopamine-modified hydrogels in wound dressing

Dopamine, a natural type of neurotransmitter, contains two phenol groups which could react with surrounding environment easily. Therefore, it is widely grafted on hydrogels to promote wound closure and provide further grafting^[23].

In previous studies, polydopamine (PDA) coating to PNIPAM hydrogel was used to increase near-infrared (NIR) response as well as promoting cell adhesion and proliferation^[24]. In addition, PDA could also conjugate with cellulose to form hydrogels, nanofibers and membranes, textiles and films in order to improve interface compatibility, interfacial stress sensitivity and crosslinking density^[25]. Dopamine could also be added to achieve self-healing property in moist environment^[26], which suggested improvement of mechanical properties as well. In this thesis, dopamine was added to modify PNIPAM-based hydrogel to broaden its applications in wound dressing.

1.3 Functional domains used in hydrogels

In this thesis, other monomers were also chosen and utilized to promote hydrogel properties.

Poly(ethylene glycol) methacrylate (PEGMA) is a high-hydrophilic polymer which could provide hydrogen bond donor groups^[27]. In this study, PEGMA was added to increase hydrophilicity of the hydrogel to achieve solubility. Acrylate-oligolactide (AOLA) could provide degradable side chains for the hydrogels^[28-31]. In addition, the transition temperature of the degradation product was increased to above 37°C, making it bioeliminable in body fluids. N-acryloxysuccinimide (NAS) could provide succinimide side groups which are

capable of conjugating to amino acids, leading to the enhanced retention of growth factors and therapeutic drugs for controlled release^[32-35]. At the same time, NAS could be applied to graft dopamine with the existence of ester bonds.

1.4 Mesenchymal stem cells used in wound dressing

Mesenchymal stem cells (MSCs) have the ability of self-renewal and multi-lineage differentiation to enhance cutaneous wound healing. Implantation of MSCs could accelerate wound closure, increase therapeutic angiogenesis, promote the regression of wound inflammation, regulate extracellular matrix remodeling, and promote skin regeneration^[36,37]. MSCs have also been proved to act as mediators in inflammatory environments, and have been applied in translational research studies^[37]. The beneficial effects of exogenous MSC on wound healing have been observed in various animal models and clinical cases^[38]. They could be injected to treat acute and chronic wounds. Therefore, MSCs were used in this study to imitate situation at wound site. In addition, MSCs were applied to test the biocompatibility of synthesized hydrogels.

1.5 Silver Nano-Coatings used as antibacterial potential for wound dressing

Bacterial inflammation has continually to be one of the urgent problems researchers need to consider when designing wound dressing materials. Several approaches have been devised, including releasing encapsulated drugs and directly using materials with inherent antibacterial activities^[39]. Among those inherent antibacterial elements, silver has been widely used due to their excellent cytotoxicity^[40]. The effectiveness of silver compounds as preservatives is based on the ability of biologically active silver ions (Ag^+) to irreversibly destroy key enzyme systems in the cell membrane of pathogens^[41]. In previous studies, Ag nanoparticles has been filled in hydrogels to improve antibacterial as well as mechanical properties by serving as secondary reinforcing agent. Ag^+ ions could also be released at controlled manner as hydrogel matrix could perform as reservoir^[42,43].

In this thesis project, conjugated dopamine on the hydrogels had oxidizing property, which could reduce silver ions to simple silver. Thus, these dopamine-modified hydrogels could be further explored as antibacterial hydrogels with the addition of silver and proper treatment.

Chapter 2: An Injectable Thermosensitive Hydrogel Potentially Used for Wound Dressing with Self-adhesive Properties

2.1 Material and methods

2.1.1 Materials

All materials included in this project were purchased from Sigma-Aldrich if not specifically mentioned.

Chemicals included in this project: N-Isopropylacrylamide (NIPAM), poly(ethylene glycol) methacrylate (PEGMA), acrylate-oligolactide (AOLA), N-acryloxysuccinimide (NAS), N-hydroxysuccinimide (NHS), benzoyl peroxide (BPO), dopamine hydrochloride (DOPA), silver nitrate (AgNO_3), sodium carbonate (Na_2CO_3), sodium sulfate (Na_2SO_4), acryloylchloride (Ac).

Solvent included in this project: dioxane, tetrahydrofuran (THF), hexane, diethyl ether, dimethylformamide (DMF), triethylamine (TEA), chloroform (CHCl_3), dichloromethane (DCM), deionized water (DI water), phosphate-buffered saline (PBS).

Materials included in cell culture: Dulbecco's modification of eagle's medium (DMEM, purchased from Corning), Minimum essential medium (MEM- α), fetal bovine serum (FBS), Trypsin serine protease enzyme (Trypsin), Penicillin streptomycin (Pen Strep).

Materials included in cell experiment: 3-(4,5-dimethylthiazol-2-yl)-2,5-diphenyltetrazolium bromide, 4',6-Diamidino-2-phenylindole dihydrochloride (DAPI), F-actin kit (purchased from acbam).

2.1.2 Synthesis of Polymer I

Four monomers were used in synthesizing polymer I, including AOLA, NAS, N-Isopropylacrylamide (NIPAM) and PEGMA. Both AOLA and NAS were synthesized through chemical reaction. N-Isopropylacrylamide (NIPAM) was purified through recrystallization before usage, and PEGMA was purified through vacuum dry.

The first step of synthesizing AOLA is combining of 45.8g lactide and 1g sodium methoxide in 10ml methanol (CH_3OH), dissolve in 100ml DCM to form poly (lactide acrylate) (PLA). The reaction is conducted under $0\text{ }^\circ\text{C}$ with nitrogen protection for 1.5 hours. After reaction, the product was washed using separating funnel with 0.1M hydrogen chloride (HCl) and brine. Then the PLA was dried with air blow overnight. Then 45g PLA was dissolved in the combination of 50ml DCM and 32.5ml TEA, 19ml acryloyl chloride (Ac) was dripped into the system. The reaction took overnight under the condition of $0\text{ }^\circ\text{C}$. After reaction finished, the product was also washed in order of 0.2M Na_2CO_3 solution, 0.1M HCl and brine for two times. Then Na_2SO_4 was added as desiccant to place overnight. The desiccant was filtered and removed through a funnel, then the product of AOLA was collected by 2 hours-lyophilization.

NAS was synthesized by adding 11.5g NHS and 11g TEA into 160ml chloroform. After dissolving them under the condition of $0\text{ }^\circ\text{C}$, 8.93ml acryloyl chloride was dripped into the system within an hour. The reaction took about 15 to 20 minutes. Then the product was washed with DI water and brine for three times. The organic solvent was dried through evaporation and the product was collected through vacuum dry.

Polymer I (poly (NIPAM-PEGMA-AOLA-NAS)) was synthesized using 1.60g NIPAM, 1.5g PEGMA, 0.283g AOLA and 0.338g NAS. The monomer ratio of synthesizing Polymer I is listed

in **Table 1**. 120ml dioxane was added to dissolve these monomers. After nitrogen protection for 20 minutes, 0.2 wt% BPO was added into the system as initiator of the reaction dropwise. Then nitrogen was ventilated for another 10 minutes. The whole reaction took 24 hours under 70 °C, 350 rpm.

The polymer was then purified after reaction. Polymer solution was dripped into 600ml cold hexane with stirring. Precipitation was formed and separated from solution using vacuum filtration. Then the filtered powder was dissolved into 20ml tetrahydrofuran (THF) and dropped into 500ml cold diethyl ether. Again, the newly formed precipitation was vacuum filtered to get the purified Polymer I. The hydrogel was collected by 24 hours-lyophilization thereafter. This Polymer I without addition of dopamine was named as D0 hydrogel.

2.1.3 Conjugation of Polymer II

Polymer II was obtained from conjugation of Polymer I and dopamine hydrochloride (DOPA). After calculating the weight ratio of NAS in Polymer I, 50% and 25% mole ratio of DOPA (70mg and 35mg) was added with 1g Polymer I into 10ml dimethylformamide (DMF). After ventilating nitrogen for 30 minutes, 68mg triethylamine (TEA) was added into the system. The conjugation took 20 hours under 60 °C.

For purification, the solvent of the polymer solution (DMF) was evaporated to dryness. Then, the residue was dissolved in 6ml THF and dripped into 150ml cold diethyl ether. The precipitation was vacuum filtered and then dissolved into 8ml THF. Again the solution was dripped into 160ml cold diethyl ether and the precipitation was filtered. The Polymer II was

collected after 24 hours vacuum dry under 60°C. Collected Polymer II were separately named as D1/4 (with 25% dopamine) and D1/2 (with 50% dopamine).

2.1.4 Chemical structure of the synthesized polymer

The structure of the synthesized polymers was confirmed through ^1H nuclear magnetic resonance (NMR) spectrum. The monomer ratio of synthetic polymers was calculated through peaks' integral.

2.1.5 Solubility, injectability and thermosensitive gelation

To test the solubility of synthesized hydrogel, 6 wt% of synthesized polymer was dissolved in PBS with continuous stirring under 4°C. Then the solution was put under 37°C to test gelation properties. To test whether the hydrogel is he injectability, the polymer solution was injected through 27 Gauze needles.

2.1.6 Water content of synthesized hydrogel

6 wt% hydrogel solution in DPBS was prepared and sterilized under UV for half an hour. Each micro centrifuge tubes were labeled and weighed w_1 . 0.2mL hydrogel solution was injected using 1mL syringe into each tube; tubes were placed in 37°C water baths for half an hour to allow gelation; 0.2mL sterilized DPBS was added as degradation medium into each

tube to replace the remaining medium after gelation. Tubes were incubated in 37°C water baths. When collecting samples at each time point, media was transferred into labelled tubes respectively and stored in -80°C freezer for degradation media cytotoxicity test. The remaining solid gels and tubes are stored in -80°C freezer. After all samples are collected, tubes with solid gel were freeze dried and weight as w_2 . Dry weight of hydrogel at each time point were calculated (w_2-w_1). The day 0 samples were incubated for at least 5 hours to allow water equilibrium in the hydrogel. Liquid was discarded and the wet weight of the gel was weight as w_3 . Following equation was used to calculate water content:

$$\text{Water content (\%)} = \frac{w_3-w_2}{w_3-w_1} * 100\%$$

2.1.7 In vitro degradation

6 wt% hydrogel solution in DPBS was prepared and sterilized under UV for half an hour. Each micro centrifuge tubes were labeled and weighed w_1 . 0.2mL hydrogel solution was injected using 1mL syringe into each tube; tubes were placed in 37°C water baths for half an hour to allow gelation; 0.2mL sterilized DPBS was added as degradation medium into each tube to replace the remaining medium after gelation. Tubes were incubated in 37°C water baths. When collecting samples at each time point, media was transferred into labelled tubes respectively and stored in -80°C freezer for degradation media cytotoxicity test. The remaining solid gels and tubes are stored in -80°C freezer. After all samples are collected, tubes with solid gel were freeze dried and weight as w_2 . Dry weight of hydrogel at each time point were calculated (w_2-w_1). Average dry weight of day0 samples was regarded as original dry weight

of the hydrogel (used for normalizing the data). Remaining weights (w_2-w_1) data were recorded at day 0, 1, 3, 7, 14, 18, 21, and 28. Data were normalized by day 0 data and the percent weight remaining curve was plotted.

2.1.8 Rheology test

Rheology test was done to determine the lower critical solution temperature (LCST). When reaches the LCST from lower temperature, the mechanical properties of polymer solution (dissolve at 4°C) would change. The test was done on AR G2 Rheometer, with a temperature increasing rate of 0.5°C per minute and temperature range from 4 to 40°C.

2.1.9 Lap shear adhesion test

The lap shear adhesion test was conducted to test the hydrogel's adhesion behavior between hydrogel, glass, and mouse skin. Mouse skin was harvest from in vivo injection experiment. After cut into pieces with an area of 2.5×3 cm, the skin was kept in 4 °C for storage and used the other day. The tissue substrates were immobilized on glass slides using cyanoacrylate glue (The Original Super Glue, purchased from Amazon)^[44]. Then the substrates were cured for 1 hour before hydrogel was attached onto it. The polymer (0.3g) was dissolved in a glass vial with an inner diameter of 2.5 mm at 4°C and put in 37°C overnight for gelation and dehydration. After taking out from vial and extra PBS taking away, the hydrogel was put onto the mouse skin and spread using a pipette tip. Then it was covered by another piece of mouse skin attached to a piece of glass slide, as shown in scheme 1. The joint area was compressed

with a weight of 85g for 30 minutes before testing. And the area attached to the skin or the glass slides was measured. This experiment was done on Instron 5583 Load Frame (controlled by Instron Bluehill software) with a stretch rate of 5mm per minute until failing. The maximum load and displacement were recorded from software and the shear strength was calculated by dividing the maximum load by the original area of hydrogel attached to skin/glass substrate. Also, a control group of glass slides was tested using the exact same method.

2.1.10 Cell culture

Cells used in this project are rat cardio fibroblasts (RCF) and rat mesenchymal stem cells (RMSC). The RCF cells were cultured with a passage number of 10-15, while RMSC cells with a passage number of 15-20.

Frozen cells were removed from liquid nitrogen environment and immediately put in 37 °C incubator to thaw. Gently swirl the vial in a 37°C water bath to quickly thaw the cells (within 1 minute) until only a small amount of ice remains in the vial. Transfer the vial to a laminar flow hood. Before opening, wipe the outside of the vial with 70% ethanol. Drop the thawed cells in T75 flasks with the addition of 9mL culture media. For RCF, the culture media was prepared using DMEM as basal. 10% FBS and 2% Pen Strep was also added. The medium was filtered through Nalgene filter (purchased from Thermo Fisher) before used to culture cells. For RMSC cells, the culturing media was prepared using MEM as basal. 10% FBS and 2% Pen Strep was also added. The medium was also filtered through Nalgene filter before usage.

The cells were cultured in the incubator with the condition of 37°C and 5% CO₂. The outside of the flasks needed to be wiped with 70% ethanol before putting into the incubator. The cell media needed to be changed when floating cells were observed through optical microscope after the adherent cells were attached to the flask bottom. Turbid media was removed with pipette. The flask was washed with 10ml PBS and twenty shakes. Then 10ml new media was added to the flask. After changing the media, flasks were put back to incubator for culturing.

Cells needed to be sub-cultured after growing for some days, as the cells were 100% attached to the flask and could be observed through microscope. For RCF cells, previous media was removed, 3ml pre-heated trypsin and 4ml PBS was added. Then the flask was put back to 37°C incubator for 5 minutes. After confirming all attached cells were detached via microscope, 3ml DMEM-based culture media was added to flask. Culturing media needed to be added quickly to balance the pH of the system, or cells could be killed. Then the total 10ml of media was transferred into a 50ml centrifuge tube. 10ml PBS was used to wash the flask and also transferred into the tube. To separate the cells from media containing trypsin, RCF cells were centrifuged under 1500 rpm for 7 minutes. After wiped with 70% ethanol, tubes were moved back into bio-safety cabinet. Media containing trypsin was removed by pipette and 3ml culture media was added into the tube. The cell-media mix was blew by pipette for 10 times for complete and evenly mixture, then 1ml mix was added to new T75 flask and another 9ml media was also added. For RMSC cells, 4ml pre-heated trypsin and 2ml PBS was added. Then the flask was put back to 37°C incubator for 4 minutes. After confirming all attached cells were detached via microscope, 4ml MEM-based culture media was added to flask. Then the total 10ml of media was transferred into a 50ml centrifuge tube. 10ml PBS was used to wash the flask and transferred into the tube. RMSC cells were centrifuged under 1600 rpm for

6 minutes. Media containing trypsin was removed by pipette and 4ml culture media was added into the tube. The cell-media mix was blew by pipette for 10 times for complete and evenly mixture, then 1ml mix was added to new T75 flask and another 9ml media was also added.

When cell growth was exceeded from needed, they could be cryopreserved. 1ml cell dispense was transferred from subculture step into cryogenic storage vials. 10% DMSO was added to each vial and the vial was put into Cryo 1°C freezing container, which could achieve a cooling rate of -1°C/min. The container was put in -80°C refrigerator overnight and transferred into liquid nitrogen environment the next day.

2.1.11 Cytotoxicity of degradation media

One way to indirectly test the cytotoxicity of the hydrogel without destroying hydrogel itself is testing MTT assay of its degradation media. Before adding media to cells, the RCF cells were digested using trypsin and PBS. After centrifuged, supernatant was removed and culture media was added back to the tube. Cell number was counted using hemacytometer through microscope, and how much it needed to be diluted was calculated. To seed on a 96 well plate, the seeding density of RCF cell was 0.01×10^6 cells per well. The cells were then cultured in 37°C for 24 hours until degradation media was added. The degradation media was collected when collecting degradation product and diluted 5 times with RCF culture media. After being irradiated under UV light for half an hour, the diluted media was added to the 96 well plate, 200µL per well, replacing the original culture media. The degradation media with degradation date of 7, 14, 21, and 28 was selected to be tested. At the same time, a control group without any treatment was also conducted to show comparison. After another culturing for 48 hours,

20 μ L 3-(4,5-dimethylthiazol-2-yl)-2,5-diphenyltetrazolium bromide solution with a concentration of 5mg/ml was added to each well. Then the plate was cultured for 4 hours before removing media carefully and wash with PBS. 200 μ L DMSO was added to each well to dissolve the reaction product of MTT solution and cell NAD(P)H-dependent oxidoreductase enzymes. After shaking carefully, the absorption spectrum of the solution was read with light wavelength of 560nm and a background of 670nm (Instrument: SpectraMax iD3).

2.1.12 Cell growth on synthesized hydrogels

How cells could grow and proliferate on synthesized hydrogel was tested through MTT and dsDNA test.

For the MTT test determining how many cells could grow on the hydrogel, 50 μ L of 6 weight percent polymer solution was added to each well of a 96-well plate, with a repeat group of 8. After completely gelation overnight, extra PBS was removed and RMSC was seeded with a seeding density of 0.01×10^6 /well, 200 μ L media per well. The timepoint of conducting MTT test was 24 and 48 hours. MTT test protocol was introduced in 2.11.

Another way to test cell growth and proliferation on hydrogel is using the PicoGreen proliferation assay, which makes use of a dye (PicoGreen) that fluoresces upon interacting with double-stranded DNA (dsDNA). The DNA is assumed to correspond directly with the number of viable cells in that sample. Cells were cultured in 96 well plate with gelled hydrogel for 1, 2, and 3 days with a repeating group of 4. When reaching testing time point, media was removed and the plate was rinsed with 200 μ L DPBS for 3 times. Then 200 μ L $1 \times$

Papain solution was added to each well and the plates were sealed with parafilm and heated at 60°C for 20 hours. The papain solution was prepared on site with 48.6ml DPBS, 625µL papain stock (10mg/ml, dissolved in DI water, purchased from), 500µL L-cystein stock (with a concentration of 200mM, dissolved in DI water), and 300µL EDTA stock (with a concentration of 333mM dissolved in DI water, pH adjusted to 8). The papain solution was restored at 4°C. After 20 hours-heating, the plates could be put in 4°C for later determination.

When all samples were collected, 50µL of TE buffer, 50µL of sample in each well, 100µL of work solution was added into a black 96 well plate. TE buffer is the combination of 10mM Tris and 1mM EDTA, pH adjusted to 8. The work solution is Picogreen (purchased from) diluted in TE buffer for 200 times. After all samples were added to the black 96 well plate, the plate was shake for 10 minutes and read by fluorescence spectrophotometer with a wavelength of 480/520 nm.

2.1.13 Cell adhesion and morphology on hydrogels

The cell growth on synthesized hydrogel was tested on 24 well plates. To determine how many cells successfully grow on the hydrogel, coverslips (Celltreat round cover glass, 15mm) were autoclaved and put at the bottom of wells for gelation. 80µL of 6% weight percent PBS polymer solution was added to each well and incubate in 37°C for at least 5 hours for complete gelation. Then the extra PBS was removed and RMSCs cells were seeded with a seeding density of 0.05×10^6 /well. After 6 and 24 hours of culturing, the plates were removed from incubator and living cells were fixed with Paraformaldehyde (PFA) for at least half an hour. Then the plate was washed with PBS for three times, with a 5 to 10 minute-shaking each time.

Then the fixed cells were stained with DAPI for 0.5 hour and F-actin for 1 hour under protection from light. After washed 3 times and shake 5 minutes each time, the coverslips were removed from 24 well plate and placed upside down on a piece of glass slides which was pre-coated with tissue mounting medium (CC/Mount™, purchased from Sigma Aldrich). The cell adhesion and morphology were observed through confocal imaging (Zeiss LSM880 Laser Scanning Confocal Microscope with Airyscan, Washington University School of Medicine).

2.1.14 Animal experiment

All animal care and use followed National Institutes of Health guidelines and Institutional Animal Care and Use Committee approval by Washington University in St Louis. C57BL/6 mice aged 8-10 weeks were used. To test the in vivo biocompatibility of synthesized hydrogel, 200µL 6% polymer solution was injected subcutaneously into the back of mouse. Besides Polymer I, Polymer II D1/4, D1/2) solution, a control group was also conducted using collagen gel as injection. After 5 days, the mice were sacrificed, and the skin of injection area was harvested. The skin was then sliced and processed with histology staining. Hematoxylin and eosin stain (H&E staining) was performed and the images were captured to show the general layout and distribution of cells along the slice direction and provide a general overview of its structure.

2.2 Results and Discussions

2.2.1 Synthesis and characterizations of hydrogels

Polymer I was synthesized through the polymerization of NIPAM, PEGMA, AOLA, NAS, as shown in **Figure 1**. The representative ^1H NMR spectra undertaken with Polymer I and II were shown in **Figure 3**. The characteristic peak at δ 4.0 ppm (d) in the spectrum represented the hydrogen atom connected to the tertiary carbon in NIPAM. The multi-peaks centered at δ 3.6 and 3.8 ppm (e, f) represented the two methylene groups brought by PEGMA. The peaks centered at δ 5.2 ppm (g) and 2.9 (h) represent the tertiary carbon in AOLA and methylene groups in NAS separately. Polymer II was synthesized through the conjugation of Polymer I and DOPA, under the condition of 60°C , N_2 protection, and TEA triggering, as shown in **Figure 2**. The multi-peaks in ^1H NMR spectrum centered at δ 6.6 ppm (j, k, l) represent the methylene groups from DOPA, meaning that dopamine hydrochloride was successfully grafted onto Polymer I. Integral also reveals that different content of dopamine was conjugated onto Polymer I. 50% and 25% dopamine were successfully grafted onto the polymer, and were named D1/2 and D1/4 hydrogel separately.

The feed ratio and real ratio of synthesized Polymer I are listed in **Table 1**. The real ratio was calculated from the integration of ^1H NMR peaks. The critical components PEGMA and NAS has the similar ratio compared with feed ratio, as PEGMA enhances the solubility of the hydrogel and NAS provides possibility of conjugating DOPA. The real conjugation ratio of DOPA is also listed in **Table 1**. The conjugated DOPA could provide further crosslinking and anti-bacterial applications.

2.2.2 Solubility, injectability and thermosensitive gelation

Solubility tests were done under 4°C, with a concentration of 6 weight percentage. 2ml of D1/2 polymer solution was placed under 4°C overnight to completely dissolve the polymer. The solubility results were shown in **Figure 4**. The polymer could dissolve well in PBS at 4°C, and gel in different times at 37°C. At the same time, it showed good injectability at 4°C when being injected through 27 Gauge needles, as performed in **Figure 5**. This good injectability of these hydrogels could provide further applications in drug delivery and tissue regeneration as medical particles could be dissolved in the solution and retained at local sites once gelled.

At lower temperatures, PNIPAM will fix itself in the solution to hydrogen bond with the water molecules that have been arranged. The water molecules must be redirected around the non-polar region of PNIPAM, which causes a decrease in entropy. At lower temperatures (such as room temperature), the negative enthalpy term produced by the hydrogen bonding effect dominates the Gibbs free energy, causing the PNIPAM to absorb water and dissolve in solution. At higher temperatures, the entropy term dominates, causing the PNIPAM to release water and phase separate.

$$\Delta G = \Delta H - T\Delta S$$

Unlike normal sol-gel transition in which subunits bond together to form a network extending throughout the whole substance ^[45], these synthesized hydrogels tended to gel with inner water drained. It's possibly due to the high hydrophilicity of PEGMA, which tended to increase entropy value therefore increase Gibbs free energy. Dopamine is also a hydrophilic

component. The addition of dopamine could increase the hydrophilicity of hydrogels and increase their solubility.

2.2.3 In vitro degradation and water content

The data of day 0, 1, 7, 14, 18, 21 and 28 was retrieved and remaining hydrogel weights were calculated and plotted against day number. As shown in **Figure 6**, the polymer degraded mainly at the ester bonds on AOLA, degrading into lactic acid. The relationship between remaining weight against degradation day number of D1/2 hydrogel and D1/4 hydrogel in **Figure 7** also revealed that these hydrogels degraded at backbone with a weight loss of around 20% after 28 days. **Figure 7** and **Table 2** showed the comparison between two hydrogels and it reveals that hydrogel with higher dopamine content (D1/2 hydrogel) could degrade relatively faster. It is possibly because of the existence of dopamine that increased the hydrophilicity of hydrogel, which promoted the reaction between hydrogel and solvent. Therefore, we could predict that the higher content dopamine the hydrogel has, the faster the hydrogel can degrade. The quick degradation also means that it will not stay for a long time at wound sites or in human tissues. It could be an advantage as some tissues require quick degradation of injected materials which would not limit wound-healing.

Water content of these hydrogels were also calculated and listed in **Table 3**. We could tell from their water content that dopamine content could increase hydrogel water content. Higher water content could resemble soft tissue property better. Therefore, proper content of dopamine could possibly promote hydrogel biocompatibility and provide more applications.

2.2.4 Rheology test

Rheology tests of synthesized hydrogels were done to determine their LCST. Because of the existence of PNIPAM, these hydrogels perform thermal-sensitivity and at LCST, their mechanical behaviors could have a sudden change. By testing their rheology behaviors, LCST could be determined and how the polymer content influence their properties could also be explored.

The rheology tests were done on AR G2 Rheometer (MEMS shared instrument group) with a temperature increase rate of 0.5°C per minute and temperature range from 4 to 40°C. In the rheology test, shear storage modulus (G') and shear loss modulus (G'') of these hydrogels against temperature were recorded. Then the ratio of loss modulus against storage modulus was calculated, which provides a measure of damping in the material.

$$\tan \delta = \frac{G''}{G'}$$

The LCST is the temperature when $\tan \delta$ suddenly changed. As listed in **Table 4**, the LCST of D0 hydrogel was 27°C, D1/4 gel was 22°C and 17°C for D1/2 hydrogel. With increasing content of dopamine, the LCST of hydrogel decreased. It was possibly because of the high hydrophilicity of dopamine that promoted reaction with solvent through hydrogen bonding, which further increased its entropy value. Therefore, these hydrogels tended to turn to entropy (ΔS) domination at lower temperature, causing the decrease of LCST. We could conclude that besides PNIPAM, dopamine could also influence the rheology behavior of thermosensitive hydrogels. With the addition of proper dopamine content, we could adjust the properties of

hydrogels to our demands, such as more convenient to storage at given temperature and more adapted to temperature required for some drugs and growth factors.

2.2.5 Lap shear adhesion tests and tissue adhesion

Lap shear adhesion strength tests were conducted to determine the lap adhesive properties of synthesized hydrogels. The hydrogels were firstly applied to glass slides as control group. As shown in **Table 5**, the shear strength of the D1/4 hydrogel was 1.87kPa and 1.91kPa for D1/2 hydrogel. Then the hydrogels were compressed between pre-cured mice skin/glass slides, as shown in **Figure 8**. The mice skin was pre-cured on glass slides with cyanoacrylate glue for 1 hour to make sure it wouldn't move on the slides. The stretch rate remained at 5mm/min and these hydrogels performed better adhesion properties than just with glass slides, as listed in **Table 5**. The lap shear strength of D1/4 hydrogel on inner layer skin was 3.93kPa and 5.13kPa on outer layer skin, while for D1/2 hydrogel was 5.40kPa on inside skin and 5.98kPa on outside skin. Because of the existence of different functional groups on both sides of skin, the hydrogels tended to form non-covalent bonds with the skin. Therefore, the lap shear strength tended to increase. At the same time, with the increasing content of dopamine, the hydrogels performed higher lap shear strength, suggesting that dopamine promoted the reactions between hydrogels and skin surfaces. It was probably because dopamine increased the amount of hydroxyl groups on the surface of hydrogels, which preferred to form hydrogen bonds with the skin and ECM. In addition, the π - π stacking might also help in the adhesion to the skin as benzene rings existed in dopamine structure as well as skin surface.

Experiments of direct adhesion between hydrogels and tissues harvested from mice were also done to test the adhesive properties to bio-tissues. As shown in **Figure 9**, both D1/4 and D1/2 hydrogels could successfully adhere to mouse heart, liver, spleen and kidney without any treatment. Hence, it could be concluded that these dopamine-modified hydrogels had good bio-adhesion properties that could be potentially used for wound dressing.

2.2.6 Cytotoxicity of degradation media

MTT assay was applied to determine the cytotoxicity of degradation media. The degradation media at day 7, 14, 21, 28 of D1/4 hydrogel was applied. The RCFs cell viability was determined through light absorbance at 560 and 670nm. As shown in **Figure 10**, cells cultured with diluted degradation media at day 7, 14, 21, 28 all had no significant difference compared with control group which had no treatment. The statistical analysis was based on t test and the p value was greater than 0.05. The results showed good cell viabilities with over 90%, as listed in **Table 6**. It meant that the degradation media of D1/4 hydrogel was non-cytotoxic to RCF cells. It could further reveal that besides degradation media, hydrogel with content of dopamine would also not restrain the RCFs growth, indicating good biocompatibility of this hydrogel and more potential biomedical applications.

2.2.7 Cell growth on hydrogels

RMSCs cells were used to test cell growth on synthesized hydrogels. Because in future work, when these hydrogels are used as wound dressing materials, stem cells could be added into the

injection to promote wound healing. Using RMSCs could imitate the condition of wound site, which could provide information of how cells would grow and proliferate at wound site with the addition of synthesized hydrogels.

One way of determining degree of cell growth on hydrogel is using MTT assay to calculate how many cells have grown on synthesized hydrogels. Also, the influence of hydrogels could also be concluded through the comparison between groups adding hydrogel and control group which had no treatment. However, the existence of hydrogel could influence the result of MTT assay. The principle of MTT solution and cells was the reaction between the NAD(P)H-dependent oxidoreductase enzymes contained by cells and tetrazolium bromide. After reaction, MTT would be reduced to formazan and turned purple. Light absorbance was based on the color change. But dopamine was also oxidant, who could react with MTT without any additional condition. The light absorbance of this reaction product was tested first. Therefore, the result could be subtracted from cell/hydrogel-MTT light absorbance. As shown in **Figure 11** and **Table 7**, with the increase of dopamine content, the light absorbance of hydrogel-MTT reaction product became stronger. It meant that hydrogels with dopamine could affect MTT assay results, as D0 hydrogel had almost no reaction with MTT solution. The light absorbance was increased with dopamine content in the hydrogels, suggesting corresponding reaction happened. The statistical analysis was based on t test. Then the MTT assays of cells grown on hydrogels were done and the effect of hydrogel-MTT was subtracted, as shown in **Figure 12** and **Table 8**. The D0 hydrogel showed low cytotoxicity to RMSCs cells. Both D1/4 and D1/2 showed good advancement of 664% and 538% separately in light absorbance, suggesting that hydrogels with dopamine could improve cell growth.

Yet the influence of dopamine-MTT reaction couldn't be completely removed. Another way to test cell growth on synthesized hydrogels was testing the double-stranded DNA (dsDNA). They could be dyed by PicoGreen dye, a fluorescent nucleic acid stain, and be quantified through fluorospectrometer. As shown in **Figure 13** and **Table 9**, at timepoint of day1 and 2, D1/2 hydrogels had improvement on cell growth. Compared with D0 hydrogel, it promoted 140-150% cell growth. It could be the reason that dopamine promoted cell adhesion and proliferation. There could be a proper content of dopamine which could improve cell growth at a maximum degree.

The result of MTT assay and dsDNA tests provided evidence that dopamine-modified hydrogels could stimulate cell growth. Thus, it could be applied to wound dressing as wound healing requires tissue regeneration, whose foundation is cell growth and proliferation.

2.2.8 Cell adhesion and morphology on hydrogels

RMSCs were seeded on pre-gelled hydrogels in 24-well plates, and then grew for 6 and 24 hours respectively to measure the cell-adhesive properties of synthesized hydrogels. At each time point, PFA was added to each well to fix cells. Then fixed cells were dyed with DAPI and F-actin for 1 hour before moved to glass slides with coverslips. As shown in **Figure 14**, cells adhere after 6 and 24 hours were fixed and imaged through confocal imaging which could capture fluorescent light from dyed cells. F-actin could be labeled to show the overall shape and structure of the cells and provide background information for other fluorescent markers. **Figure 14 (a)-(c)** suggested that after 6 hours, compared with number of cells grown on D1/4 hydrogel, more cells were attached and spread on D1/2 gel as cells grown on D0

hydrogel remained round shape. **Figure 14 (d)-(f)** showed that after 24 hours, both D1/4 and D1/2 hydrogels performed better cell adhesion compared with hydrogel without any dopamine (D0 hydrogel). Also, cell morphology in **Figure 14 (f)** suggested that D1/2 hydrogel improved the spreading ability of cells significantly. With the increasement of dopamine content, cells were more likely to attach on substrates. Therefore, it could be concluded that dopamine could promote cell adhesion and could be applied in wound dressing to accelerate tissue regeneration and wound healing.

2.2.9 In vivo biocompatibility

H&E staining is the combination of hematoxylin and eosin stain. The hematoxylin stains cell nuclei blue, and eosin stains the extracellular matrix and cytoplasm pink, with other structures taking on different shades, hues, and combinations of these colors^[46]. 5 days after the subcutaneous injection of the hydrogel, the mice were sacrificed, and the skin of injection area was harvested. The skin was then sliced and processed with histology staining. Then the staining results were observed through optical microscope under the magnification of 10× and 20×, as shown in **Figure 15-19**. **Figure 15** showed the 10×magnificence image of stained slices. In this figure, the white area without any cells or tissue could be the location of subcutaneous injection. It meant that after only 5 days of injection, there were still hydrogel residue. Acute inflammation after injection could also be observed. Collagen gel has been widely used for subcutaneous injection as carrier of donor cells and implantation^[47]. In **Figure 17**, which showed slices 5 days after D0 hydrogel injection, hydrogel residue was observed between epidermis and dermis layer. It performed no significant difference with control group,

indicating low in vivo toxicity. **Figure 18** and **Figure 19** were skin slices after 5 days injection of D1/4 and D1/2 hydrogels, respectively. Both D1/4 and D1/2 hydrogels performed similar in vivo toxicity compared with collagen gel, which had already been proved to be harmless. Thus, D1/4 and D1/2 hydrogels could potentially be applied as drug carriers and adhesives in wound healing.

2.3 Conclusions

In this thesis, thermosensitive hydrogels with different content of dopamine were synthesized and different properties were tested. These dopamine-modified hydrogels performed good solubility and injectability, as well as high water content and good degradability. The increasing content of dopamine could improve the hydrophilicity of synthesized hydrogels, therefore brought lower LCST, higher water content and faster degradation. In addition, dopamine on these hydrogels could modify adhesive properties. Thus, these hydrogels performed higher lap shear strength and promoted cell adhesion and proliferation. The degradation media of these DOPA-modified hydrogels also showed low cytotoxicity, which meant good in vitro biocompatibility. Furthermore, these hydrogels behaved rather good in vivo biocompatibility after subcutaneously injected into mice. Therefore, it could be concluded that these dopamine-modified thermosensitive hydrogels could utilized as wound dressing to advance wound healing through direct adhesion and assistance of tissue regeneration.

Chapter 3: Future work

3.1 Further improvements of hydrogel properties

The synthesized hydrogels could promote cell adhesion and proliferation. However, the mechanical properties need to be modified by rather adjusting monomer ration or addition of secondary crosslinker. Moreover, long-time biocompatibility and in vivo degradation should be tested to determine whether these hydrogels could be utilized in chronic wound healing. The ability of drug or cell loading of these DOPA-modified hydrogels could also be tested in future studies.

3.2 Antibacterial Ag-coated dopamine hydrogel

Silver particles could be reduced from ions by oxidizing DOPA. Further experiments exploring how silver particles would work on these DOPA-modified hydrogels need to be conducted, such as influence of Ag concentration and in vitro antibacterial estimation. Also, silver particles coated onto DOPA-modified hydrogels in this thesis were indeterminate. Thus, silver nanoparticles (AgNPs) could be further applied to improve the antibacterial properties of hydrogels. AgNPs' loading and releasing could be the next steps of applying these hydrogels into wound dressing.

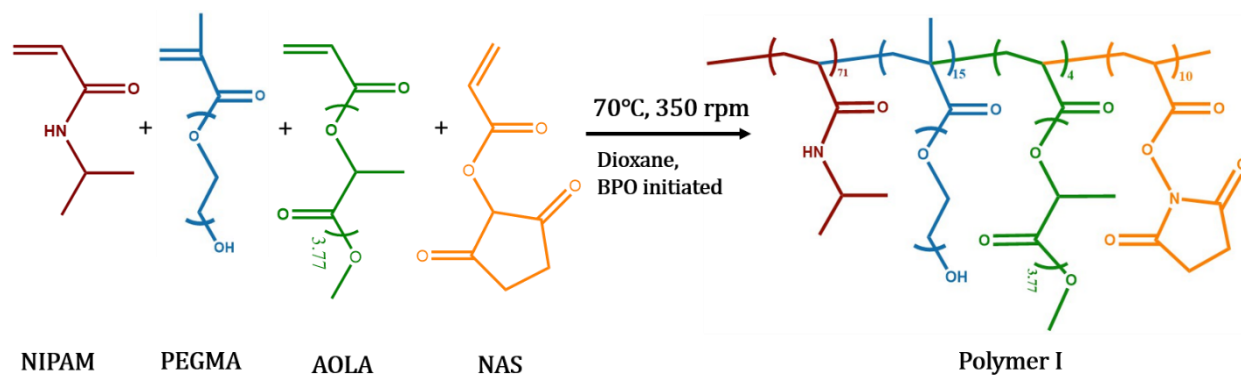
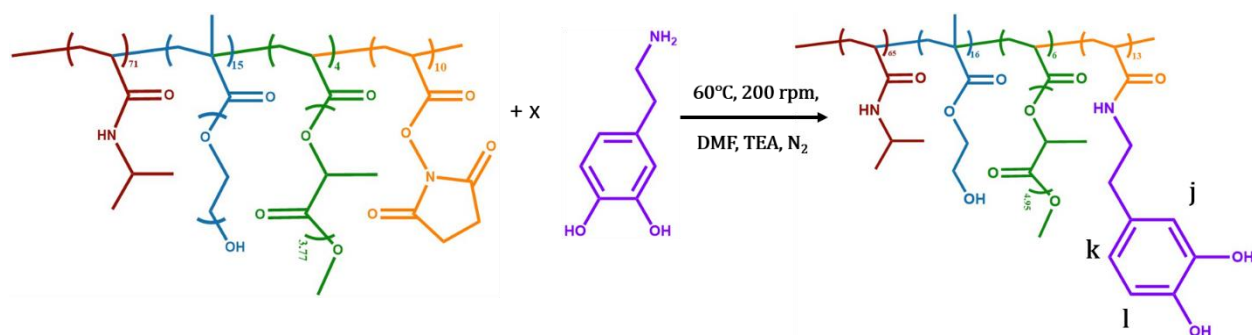


Figure 1. Synthesis of Polymer I.

Figure 2. Conjugation of Polymer II. $x=0.25, 0.5$.

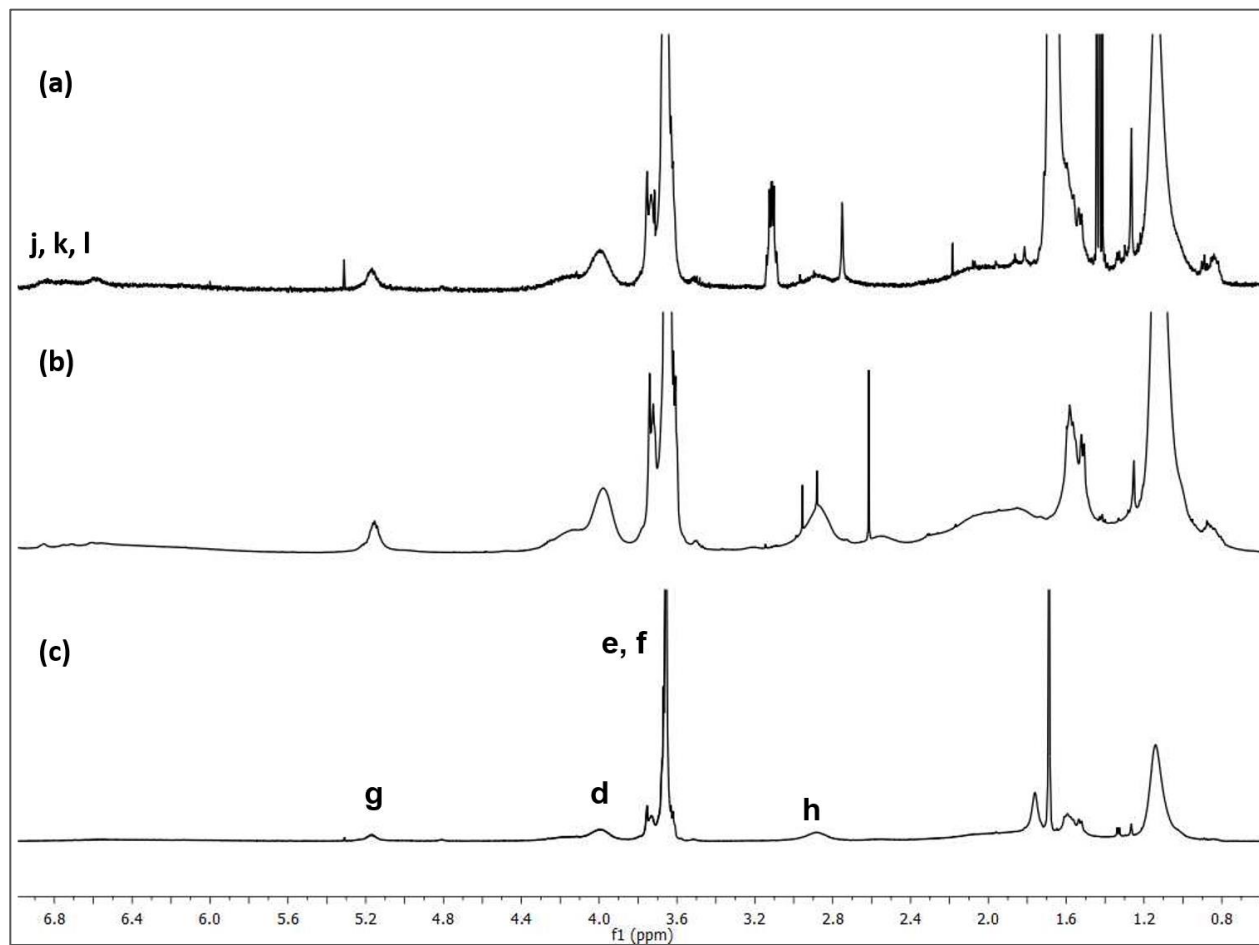


Figure 3. ^1H NMR spectrum of synthesized polymer. (a) Polymer II, D1/2 hydrogel; (b) Polymer II, D1/4 hydrogel; (c) Polymer I, D0 hydrogel.

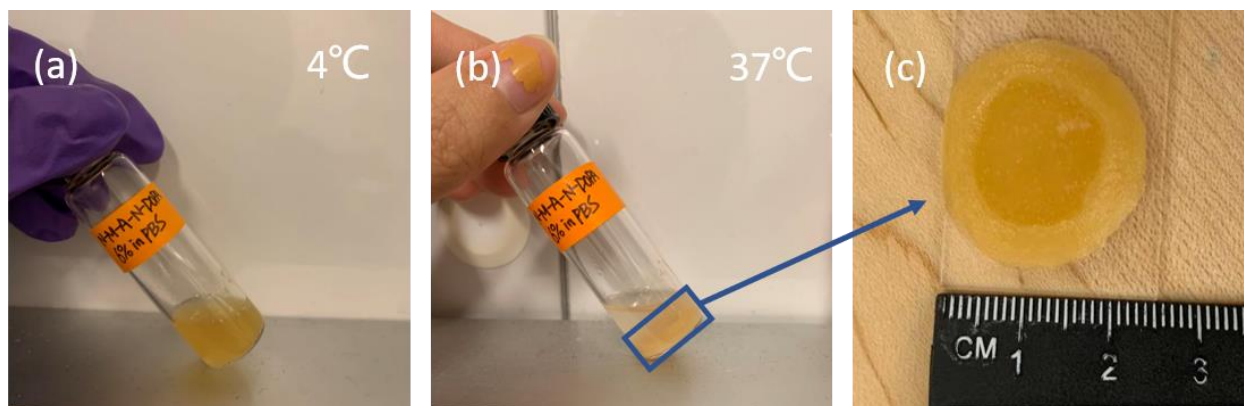


Figure 4. Solubility of synthesized polymers. (a) D0 hydrogel, (b) D1/4 hydrogel, and (c) D1/2 hydrogel. All dissolved at 4°C and gelled at 37°C.

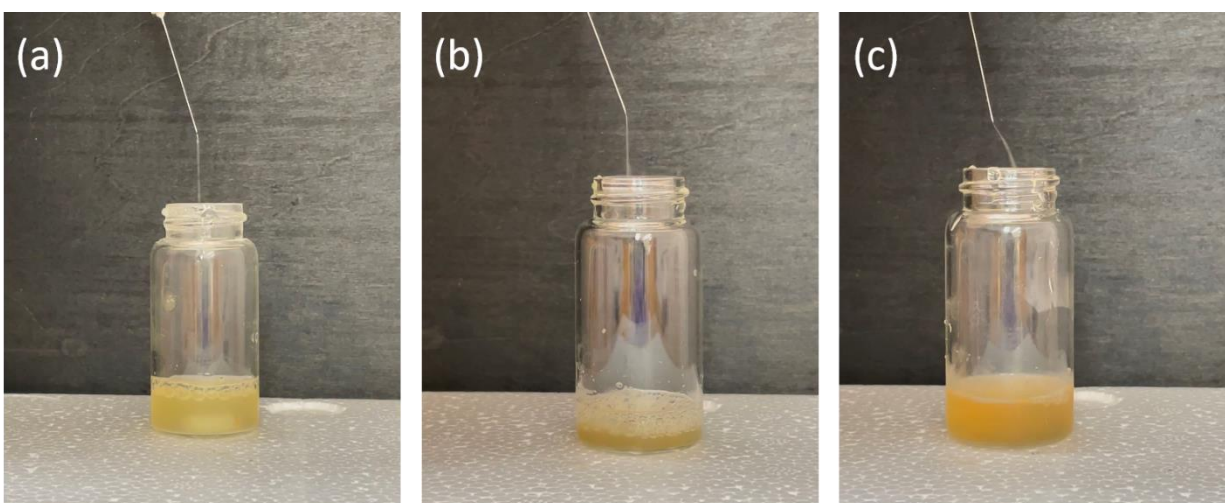


Figure 5. Injectability of synthesized polymers through 27 Gauge needles, at 4°C. (a) D0 hydrogel, (b) D1/4 hydrogel, and (c) D1/2 hydrogel.

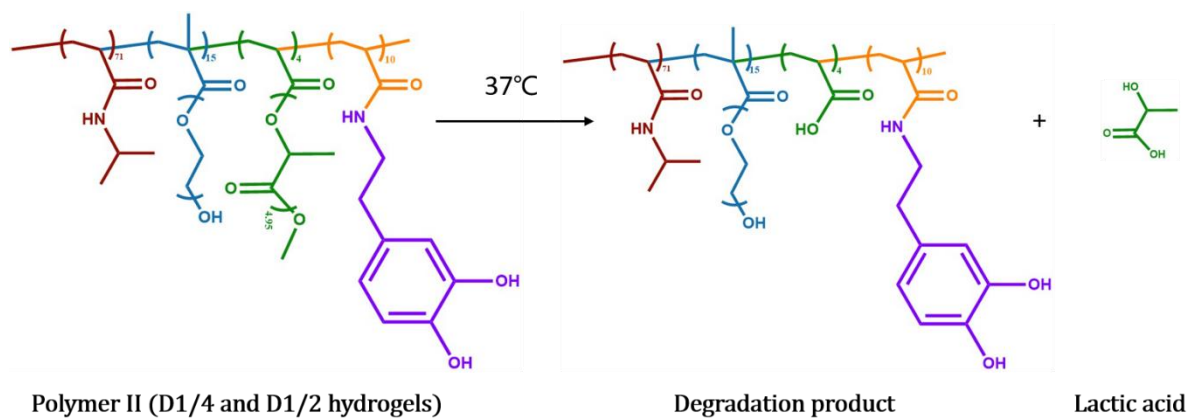


Figure 6. Schematic illustration of degradation product of Polymer II.

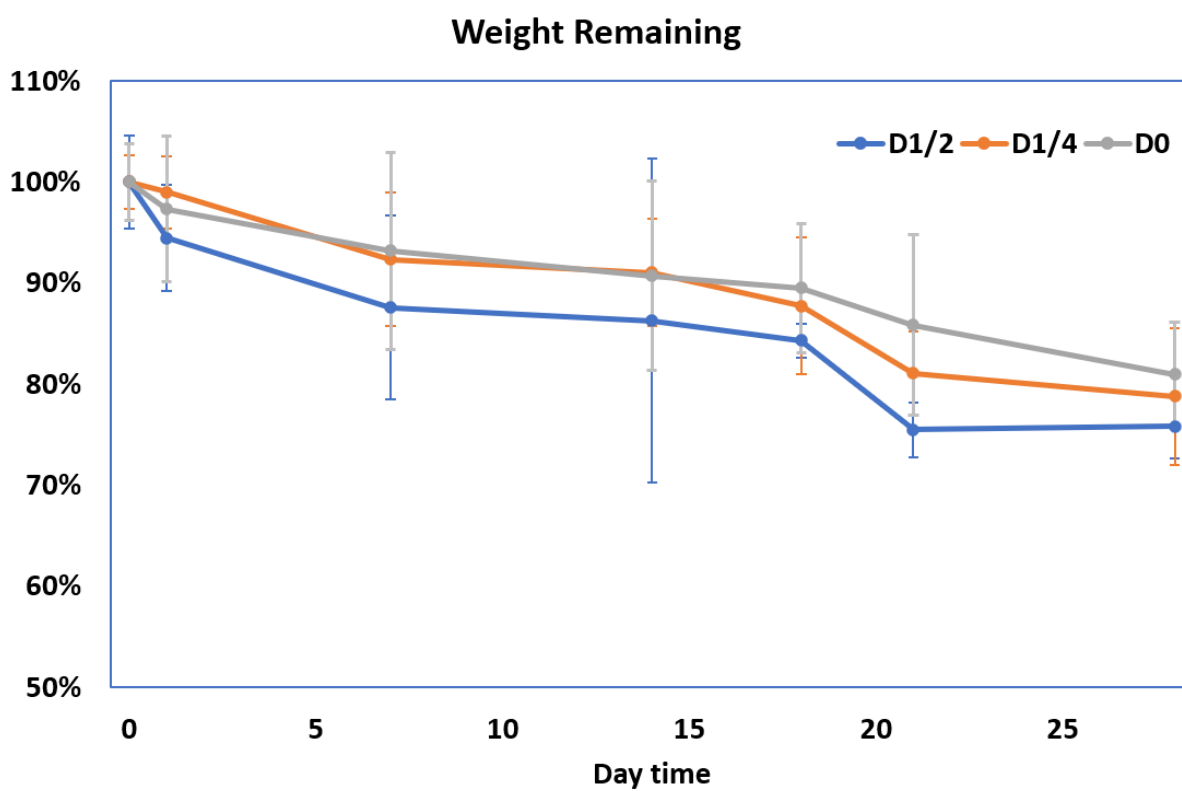


Figure 7. Degradation of D1/4 and D1/2 hydrogels.

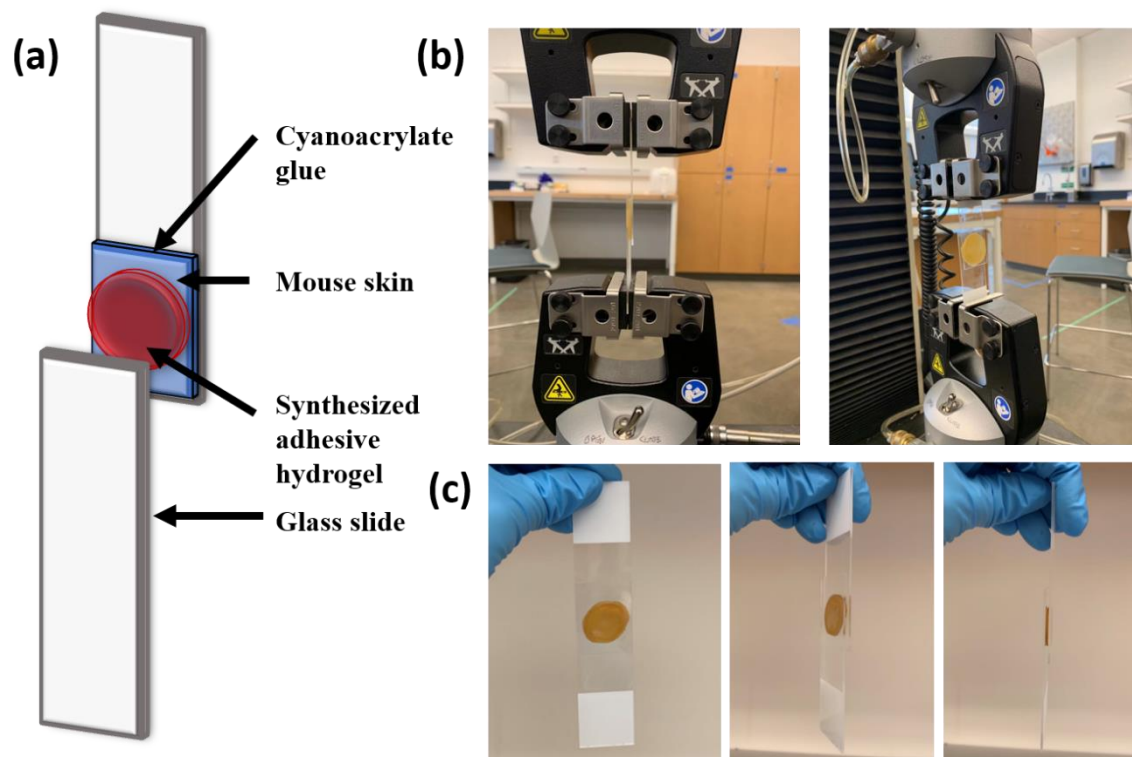


Figure 8. (a) Schematic illustration of lap shear adhesion tests. (b) Instron used to test the lap shear strength. (c) Direct adhesion between hydrogel and glass slides.

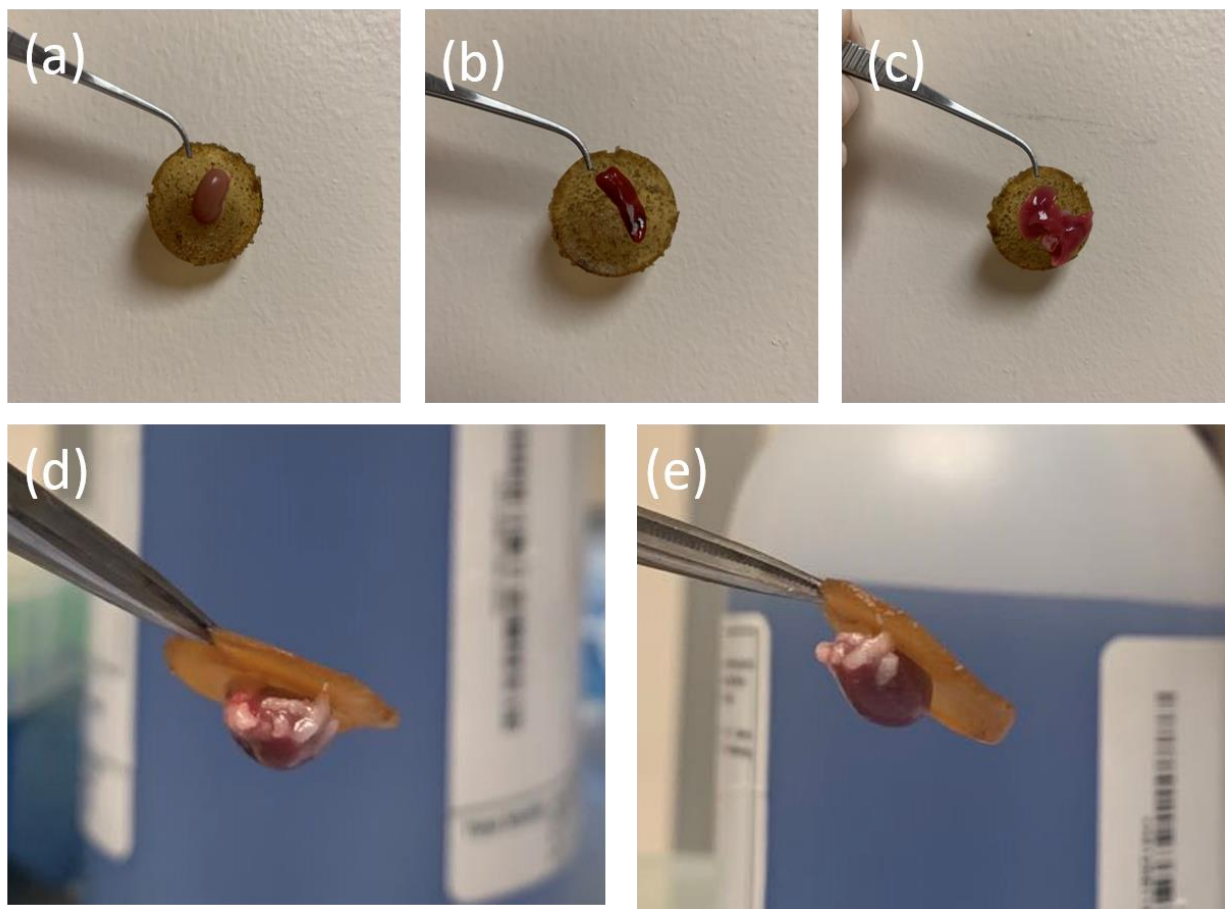


Figure 9. Adhesion between hydrogels and tissues. (a) D1/4 hydrogel with mouse kidney, (b) D1/4 hydrogel with mouse spleen, (c) D1/4 hydrogel with mouse liver; (d) D1/2 hydrogel with mouse heart, (e) D1/2 hydrogel with mouse kidney.

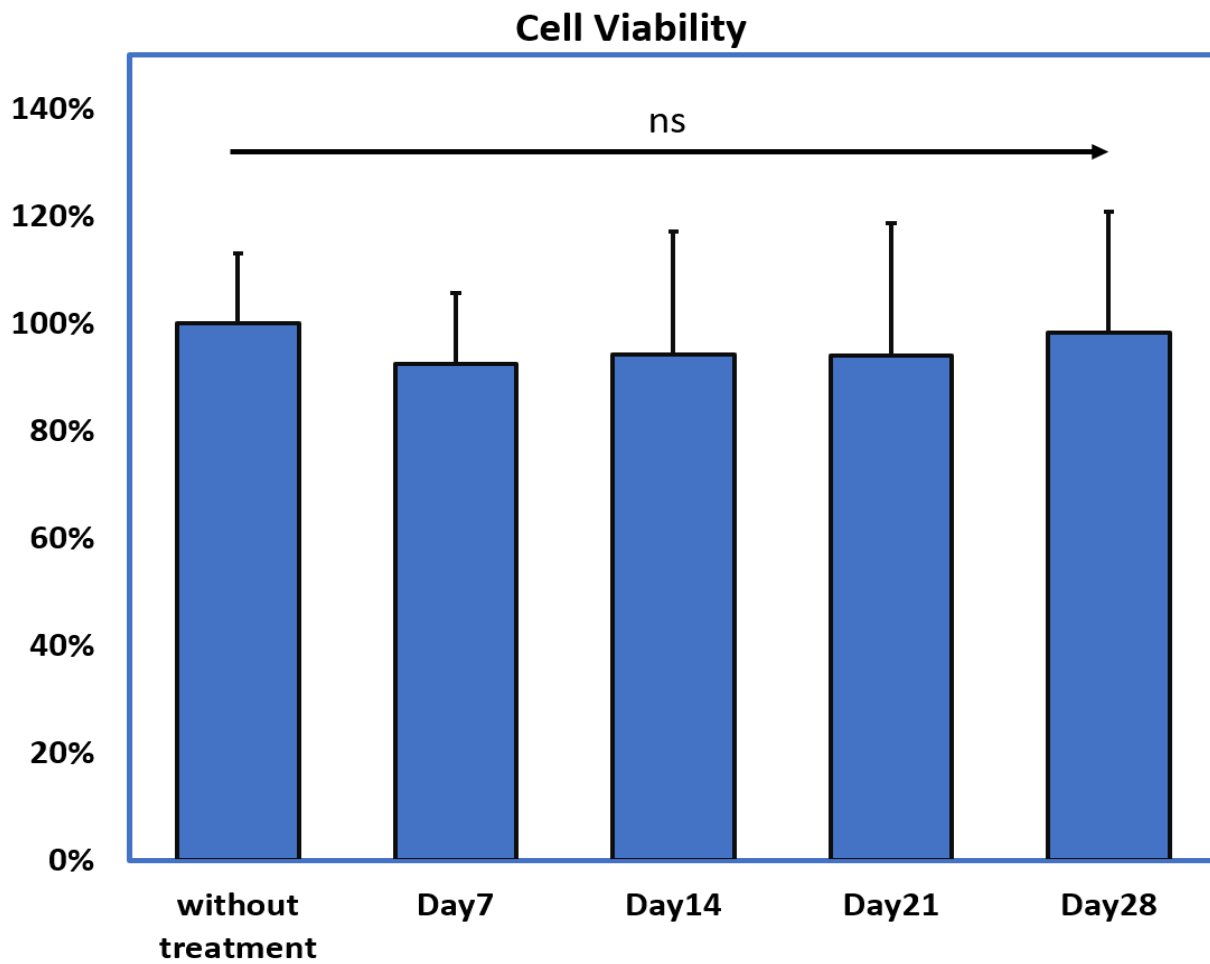


Figure 10. Cytotoxicity of degradation medium. Cell viability of day 7, 14, 21, 28 degradation media. n=8, ns: $p \geq 0.05$.

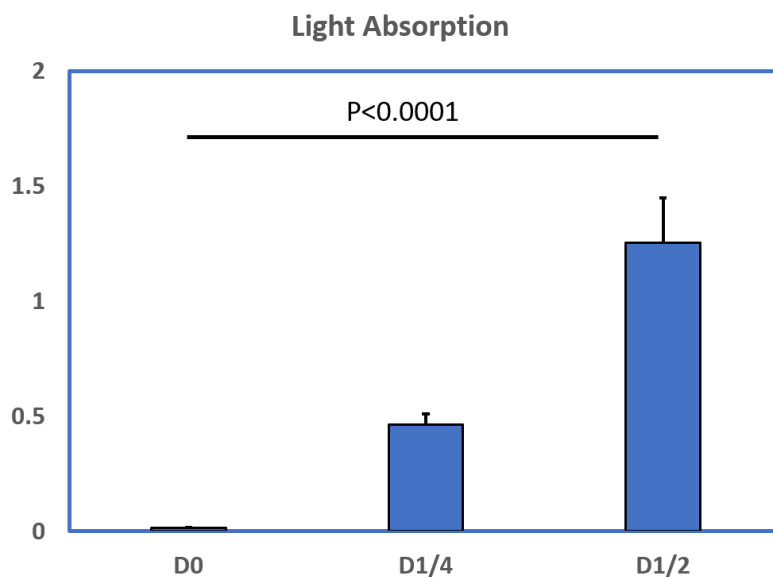


Figure 11. Reaction between hydrogels and MTT solution. Absorbance spectrum of reaction product at 560 and 670 nm. n=8.

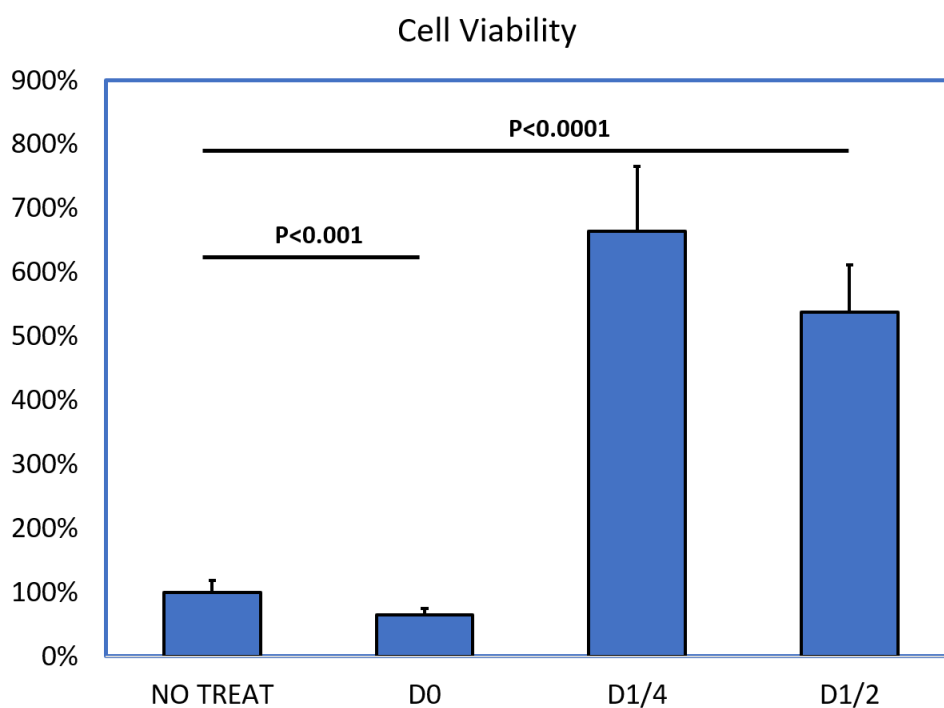


Figure 12. MTT assay of RMSCs growth on synthesized hydrogels. Absorbance spectrum of MTT assay at 560 and 670 nm, influence of dopamine-MTT solution reaction is removed. n=8.

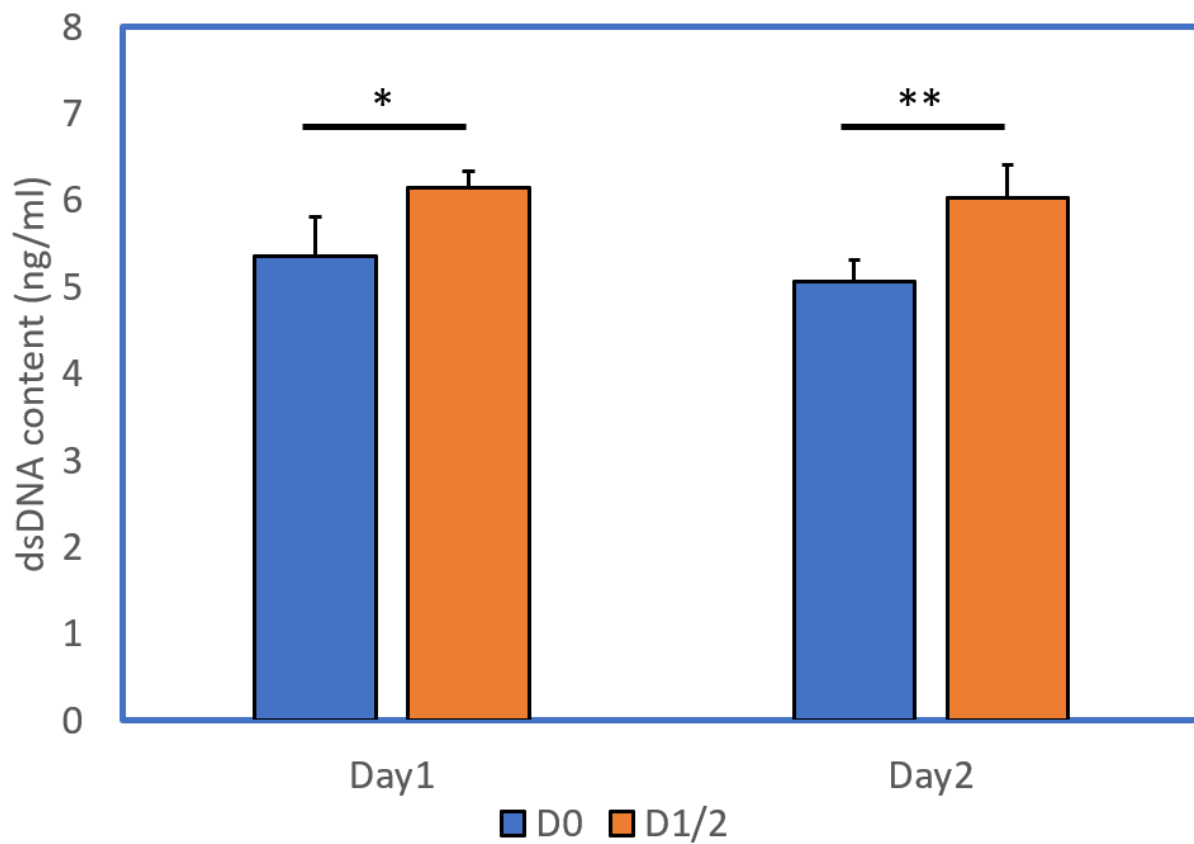


Figure 13. Cell growth on synthesized hydrogels. dsDNA test of RMSCs growing on no treatment coverslip, D0 and D1/2 hydrogels after 1 and 2 days. n=4, *: $p < 0.05$, **: $p < 0.01$.

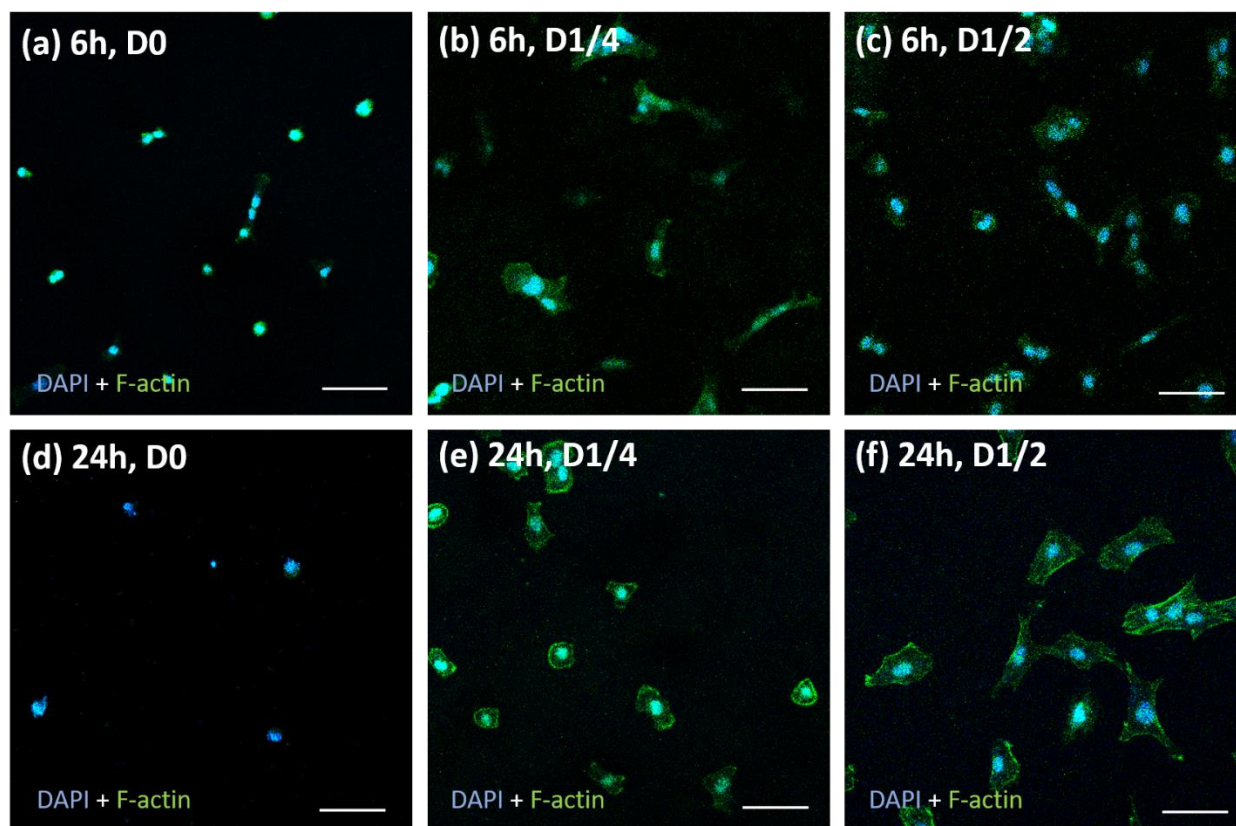


Figure 14. Image of cell adhesion on hydrogels. (a)-(c) Confocal imaging of RMSCs grew on D0, D1/4 and D1/2 hydrogels after 6 hours; (d)-(f) RMSCs grew on D0, D1/4 and D1/2 hydrogels after 24 hours. Scale bar: 50 μ m.

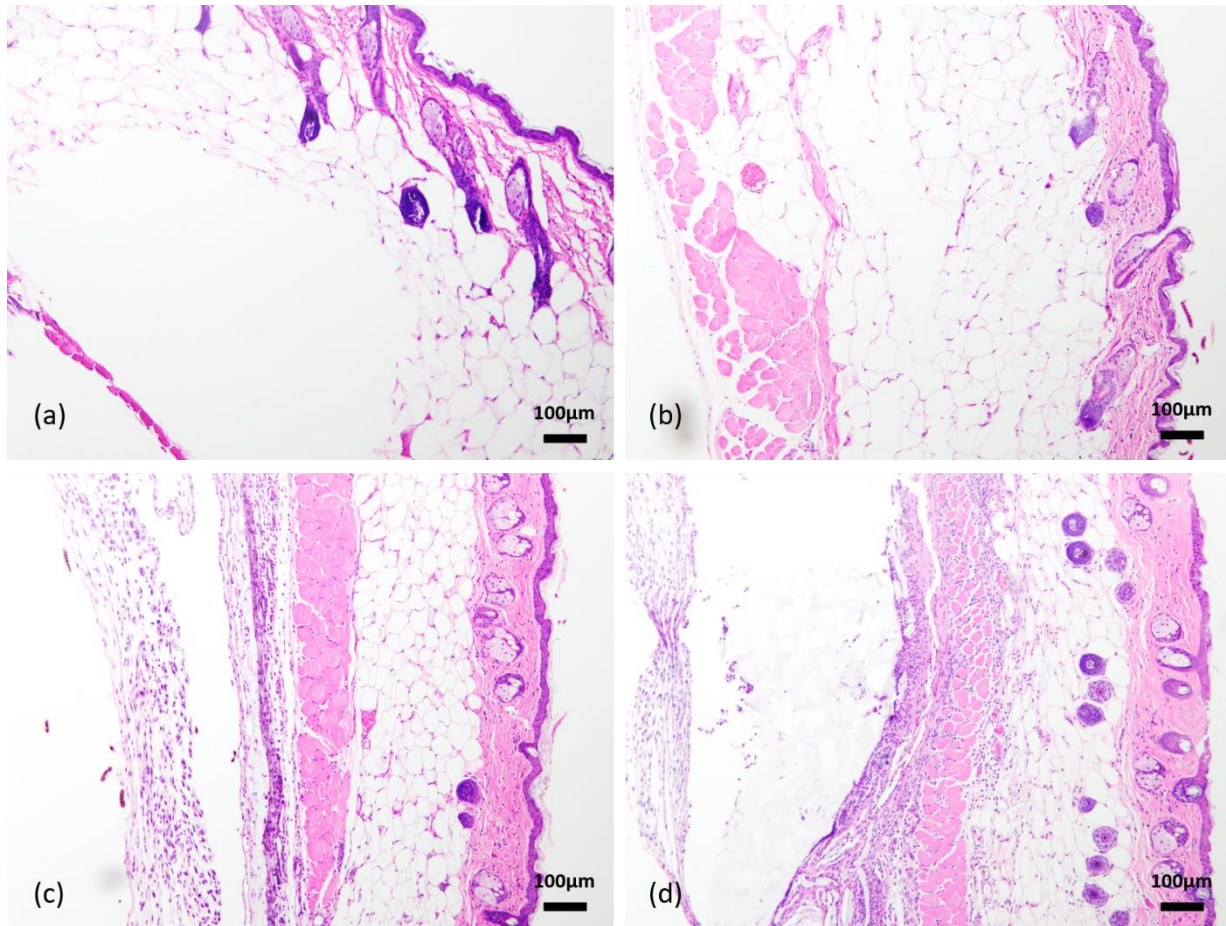


Figure 15. 10× imaging of H&E staining after 5 days of subcutaneous injection skin slices. (a) Control group injected with collagen gel, (b) injected with D0 hydrogel, (c) injected with D1/4 hydrogel, and (d) D1/2 hydrogel. Scale bar: 100µm

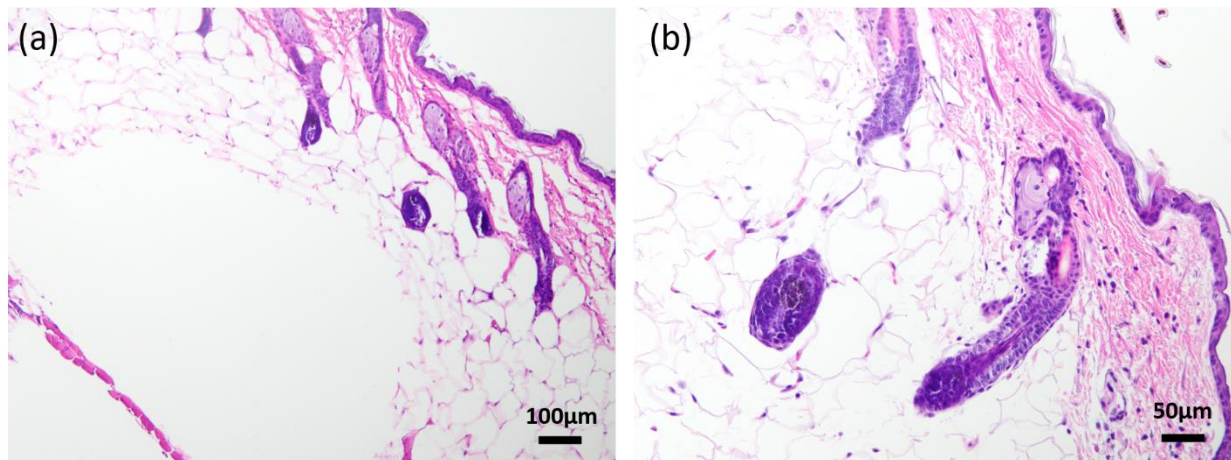


Figure 16. H&E staining of subcutaneous injection samples, control group injected with collagen hydrogel. (a) 10× and (b) 20× magnification imaging of slices.

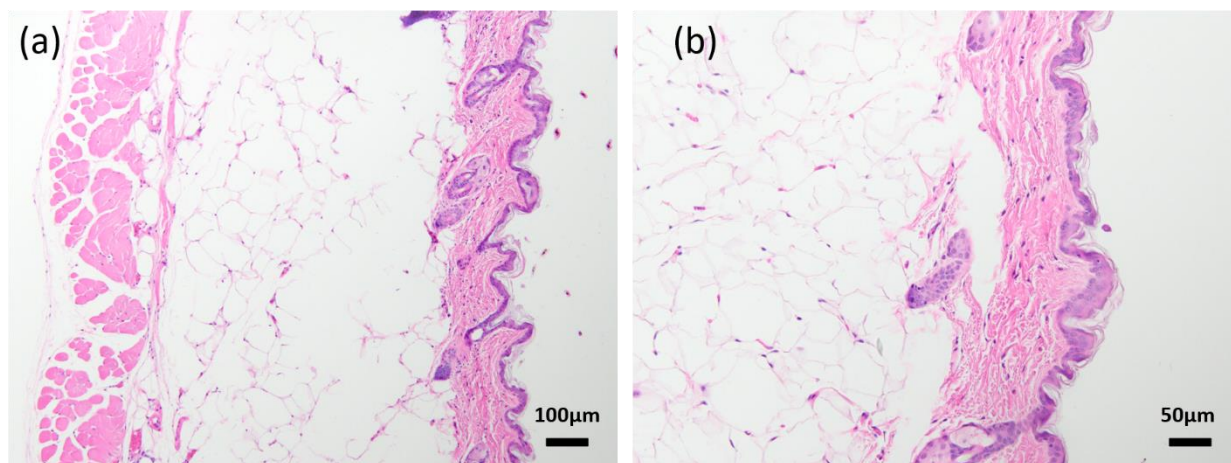


Figure 17. H&E staining of subcutaneous injection samples, 200 μ L Polymer I solution (D0 hydrogel) injected. (a) 10× and (b) 20× magnification imaging of slices.

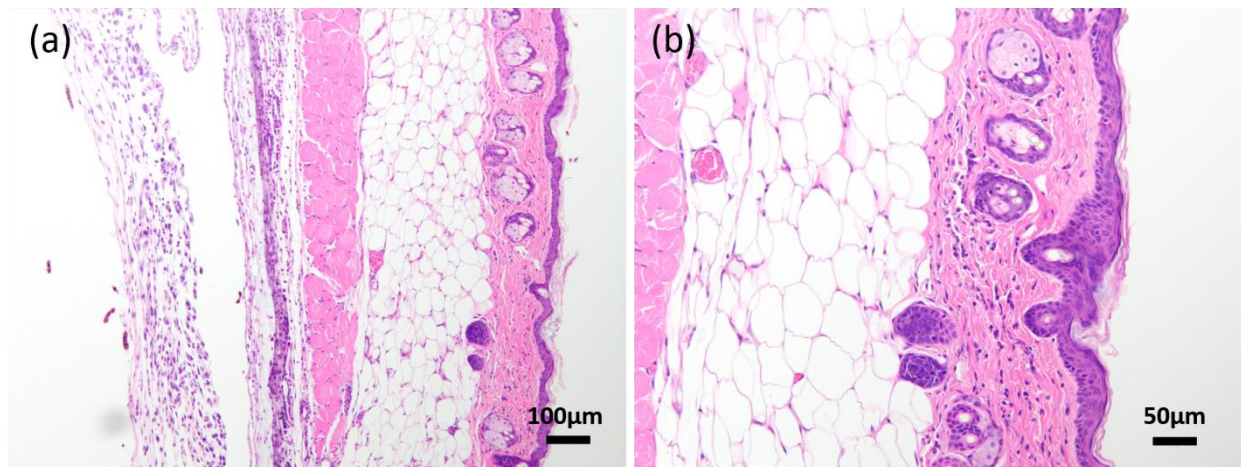


Figure 18. H&E staining of subcutaneous injection samples, Polymer II solution (D1/4 hydrogel) injected with collagen hydrogel. (a) 10× and (b) 20× magnification imaging of slices.

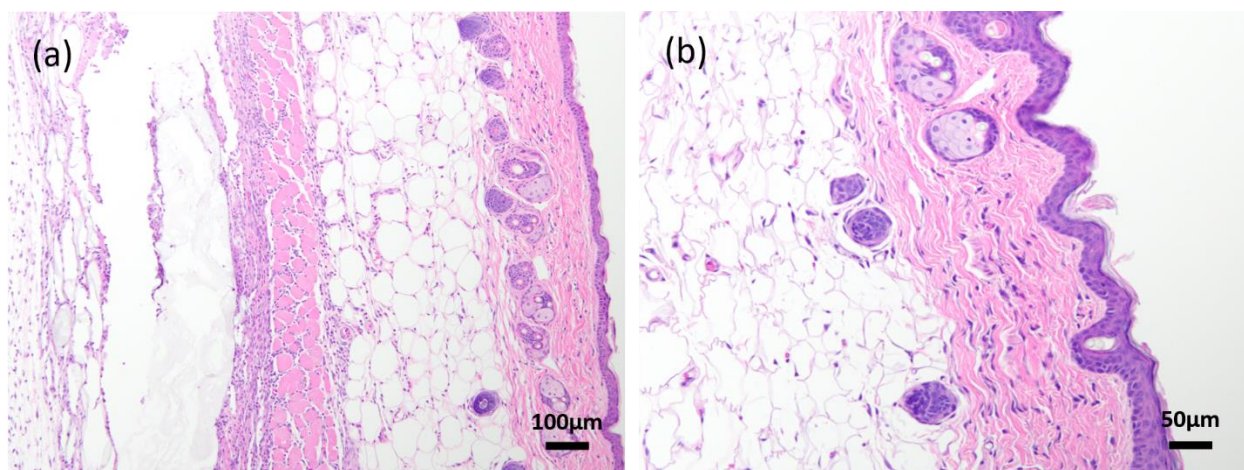


Figure 19. H&E staining of subcutaneous injection samples, Polymer II solution (D1/2 hydrogel) injected with collagen hydrogel. (a) 10× and (b) 20× magnification imaging of slices.

Table 1

Feed ratio and real ratio of synthesized Polymer I and Polymer II.

		Monomer				
		NIPAM	PEGMA	AOLA	NAS	DOPA
Polymer I	Feed ratio	71	15	4	10	
	Real ratio	65	16	6	13	
Polymer II	D1/4 Feed ratio				1	0.3
	Real ratio				1	0.23
	D1/2 Feed ratio				1	0.6
	Real ratio				1	0.53

Table 2

Degradation remaining weight of synthesized hydrogels.

	D1/2 hydrogel		D1/4 hydrogel	
	Weight remaining	Standard deviation	Weight remaining	Standard deviation
Day0	100.00%	4.58%	100.00%	2.65%
Day1	94.44%	5.27%	98.98%	3.61%
Day3	93.46%	8.70%	89.77%	4.51%
Day7	87.58%	9.12%	92.33%	6.62%
Day14	86.27%	16.05%	91.05%	5.33%
Day18	84.31%	1.69%	87.72%	6.77%
Day21	75.49%	2.69%	81.07%	4.13%
Day28	75.82%	3.20%	78.77%	6.81%

Table 3

Water content of synthesized hydrogels.

Hydrogel	Water content	Standard deviation
D0	72.3%	7.08%
D1/4	77.37%	4.32%
D1/2	85.94%	2.17%

Table 4

LCST of synthesized hydrogels.

Dopamine content	LCST (°C)
0	27
0.25	22
0.5	17

Table 5

Lap shear strength of D1/4 and D1/2 hydrogels.

	Glass slide (kPa)	Inside skin / Glass (kPa)	Outside skin / Glass (kPa)
D1/4	1.86963	3.9165	5.12843
D1/2	1.9123	5.39856	5.98436

Table 6

Cell viability percentage of MTT assay of RCFs growing on synthesized hydrogels.

	Without treatment	Day7	Day14	Day21	Day28
Average percentage	100%	93%	94%	94%	98%
Standard deviation	10.96%	6.68%	7.12%	12.59%	6.59%

Table 7

Light absorbance of reaction product of D1/4 and D1/2 hydrogels with MTT solution.

	D0	D1/4	D1/2
Average absorbance	0.01525	0.464875	1.253
Standard Deviation	0.002605	0.045423	0.197174

Table 8

Light absorbance of RMSCs MTT assay with dopamine-MTT solution reaction influence removed.

	NO TREAT	D0	D1/4	D1/2
Average	100.00%	64.64%	663.98%	537.73%
Standard Deviation	19.03%	9.70%	101.39%	74.38%

Table 9

Proportion of fluorescence absorbance of cell growth on synthesized hydrogels

	D0		D1/2	
	Average growth	SD	Average growth	SD
Day1	100.00%	27.14%	146.68%	11.08%
Day2	82.39%	15.05%	140.09%	22.44%
Day3	116.73%	18.22%	150.44%	7.13%

References

1. Kokabi, M., Sirousazar, M., & Hassan, Z. M. (2007). PVA–clay nanocomposite hydrogels for wound dressing. *European Polymer Journal*, 43(3), 773–781.
<https://doi.org/10.1016/j.eurpolymj.2006.11.030>
2. Rujitanaroj, P., Pimpha, N., & Supaphol, P. (2008). Wound-dressing materials with antibacterial activity from electrospun gelatin fiber mats containing silver nanoparticles. *Polymer*, 49(21), 4723–4732. <https://doi.org/10.1016/j.polymer.2008.08.021>
3. Azad, A. K., Sermsintham, N., Chandkrachang, S., & Stevens, W. F. (2004). Chitosan membrane as a wound-healing dressing: Characterization and clinical application. *Journal of Biomedical Materials Research*, 69B(2), 216–222.
<https://doi.org/10.1002/jbm.b.30000>
4. Dhivya, S., Padma, V. V., & Santhini, E. (2015). Wound dressings – a review. *BioMedicine*, 5(4). <https://doi.org/10.7603/s40681-015-0022-9>
5. Ajji, Z., Othman, I., & Rosiak, J. M. (2005). Production of hydrogel wound dressings using gamma radiation. *Nuclear Instruments and Methods in Physics Research Section B: Beam Interactions with Materials and Atoms*, 229(3), 375–380.
<https://doi.org/10.1016/j.nimb.2004.12.135>
6. Razzak, M. T., Darwis, D., Zainuddin, & Sukirno. (2001). Irradiation of polyvinyl alcohol and polyvinyl pyrrolidone blended hydrogel for wound dressing. *Radiation Physics and Chemistry*, 62(1), 107–113. [https://doi.org/10.1016/S0969-806X\(01\)00427-3](https://doi.org/10.1016/S0969-806X(01)00427-3)
7. Balakrishnan, B., Mohanty, M., Umashankar, P. R., & Jayakrishnan, A. (2005). Evaluation of an in situ forming hydrogel wound dressing based on oxidized alginate and gelatin. *Biomaterials*, 26(32), 6335–6342. <https://doi.org/10.1016/j.biomaterials.2005.04.012>
8. *All-natural injectable hydrogel with self-healing and antibacterial properties for wound dressing* | SpringerLink. (n.d.). Retrieved April 10, 2021, from <https://link.springer.com/article/10.1007/s10570-019-02942-8>

9. Zhao, X., Wu, H., Guo, B., Dong, R., Qiu, Y., & Ma, P. X. (2017). Antibacterial anti-oxidant electroactive injectable hydrogel as self-healing wound dressing with hemostasis and adhesiveness for cutaneous wound healing. *Biomaterials*, *122*, 34–47.
<https://doi.org/10.1016/j.biomaterials.2017.01.011>
10. Gong, C., Wu, Q., Wang, Y., Zhang, D., Luo, F., Zhao, X., Wei, Y., & Qian, Z. (2013). A biodegradable hydrogel system containing curcumin encapsulated in micelles for cutaneous wound healing. *Biomaterials*, *34*(27), 6377–6387.
<https://doi.org/10.1016/j.biomaterials.2013.05.005>
11. *In Situ Forming and Rutin-Releasing Chitosan Hydrogels As Injectable Dressings for Dermal Wound Healing | Biomacromolecules*. (n.d.). Retrieved April 10, 2021, from <https://pubs.acs.org/doi/10.1021/bm200326g>
12. Mathew, A. P., Uthaman, S., Cho, K.-H., Cho, C.-S., & Park, I.-K. (2018). Injectable hydrogels for delivering biotherapeutic molecules. *International Journal of Biological Macromolecules*, *110*, 17–29. <https://doi.org/10.1016/j.ijbiomac.2017.11.113>
13. Xu, Q., A, S., Gao, Y., Guo, L., Creagh-Flynn, J., Zhou, D., Greiser, U., Dong, Y., Wang, F., Tai, H., Liu, W., Wang, W., & Wang, W. (2018). A hybrid injectable hydrogel from hyperbranched PEG macromer as a stem cell delivery and retention platform for diabetic wound healing. *Acta Biomaterialia*, *75*, 63–74.
<https://doi.org/10.1016/j.actbio.2018.05.039>
14. Qu, J., Zhao, X., Ma, P. X., & Guo, B. (2017). PH-responsive self-healing injectable hydrogel based on N-carboxyethyl chitosan for hepatocellular carcinoma therapy. *Acta Biomaterialia*, *58*, 168–180. <https://doi.org/10.1016/j.actbio.2017.06.001>
15. *Bioinspired pH- and Temperature-Responsive Injectable Adhesive Hydrogels with Polyplexes Promotes Skin Wound Healing | Biomacromolecules*. (n.d.). Retrieved April 10, 2021, from https://pubs.acs.org/doi/abs/10.1021/acs.biomac.8b00819?casa_token=mhN_R3JJ19IAA AAA:yD1uSD2t_70p1wIPfVMBZmVEHSFIuwRydM7n7XHkBkLYtHD0Irqby4vX3sp SVO6c0ydjDAUyuzjMEtM

16. Zubik, K., Singhsa, P., Wang, Y., Manuspiya, H., & Narain, R. (2017). Thermo-Responsive Poly(N-Isopropylacrylamide)-Cellulose Nanocrystals Hybrid Hydrogels for Wound Dressing. *Polymers*, 9(4), 119. <https://doi.org/10.3390/polym9040119>
17. Gao, S., Ge, W., Zhao, C., Cheng, C., Jiang, H., & Wang, X. (2015). Novel conjugated Ag@PNIPAM nanocomposites for an effective antibacterial wound dressing. *RSC Advances*, 5(33), 25870–25876. <https://doi.org/10.1039/C5RA01199J>
18. Vihola, H., Laukkanen, A., Valtola, L., Tenhu, H., & Hirvonen, J. (2005). Cytotoxicity of thermosensitive polymers poly(N-isopropylacrylamide), poly(N-vinylcaprolactam) and amphiphilically modified poly(N-vinylcaprolactam). *Biomaterials*, 26(16), 3055–3064. <https://doi.org/10.1016/j.biomaterials.2004.09.008>
19. Li, M., Liang, Y., He, J., Zhang, H., & Guo, B. (2020). Two-Pronged Strategy of Biomechanically Active and Biochemically Multifunctional Hydrogel Wound Dressing To Accelerate Wound Closure and Wound Healing. *Chemistry of Materials*, 32(23), 9937–9953. <https://doi.org/10.1021/acs.chemmater.0c02823>
20. Fan, Z., Xu, Z., Niu, H., Gao, N., Guan, Y., Li, C., Dang, Y., Cui, X., Liu, X. L., Duan, Y., Li, H., Zhou, X., Lin, P.-H., Ma, J., & Guan, J. (2018). An Injectable Oxygen Release System to Augment Cell Survival and Promote Cardiac Repair Following Myocardial Infarction. *Scientific Reports*, 8(1), 1371. <https://doi.org/10.1038/s41598-018-19906-w>
21. Chen, S., Shi, J., Xu, X., Ding, J., Zhong, W., Zhang, L., Xing, M., & Zhang, L. (2016). Study of stiffness effects of poly(amidoamine)–poly(n-isopropyl acrylamide) hydrogel on wound healing. *Colloids and Surfaces B: Biointerfaces*, 140, 574–582. <https://doi.org/10.1016/j.colsurfb.2015.08.041>
22. Ha, D. I., Lee, S. B., Chong, M. S., Lee, Y. M., Kim, S. Y., & Park, Y. H. (2006). Preparation of thermo-responsive and injectable hydrogels based on hyaluronic acid and poly(N-isopropylacrylamide) and their drug release behaviors. *Macromolecular Research*, 14(1), 87–93. <https://doi.org/10.1007/BF03219073>

23. Zhang, H., Sun, X., Wang, J., Zhang, Y., Dong, M., Bu, T., Li, L., Liu, Y., & Wang, L. (n.d.). Multifunctional Injectable Hydrogel Dressings for Effectively Accelerating Wound Healing: Enhancing Biomineralization Strategy. *Advanced Functional Materials*, *n/a(n/a)*, 2100093. <https://doi.org/10.1002/adfm.202100093>
24. Han, L., Zhang, Y., Lu, X., Wang, K., Wang, Z., & Zhang, H. (2016). Polydopamine Nanoparticles Modulating Stimuli-Responsive PNIPAM Hydrogels with Cell/Tissue Adhesiveness. *ACS Applied Materials & Interfaces*, *8(42)*, 29088–29100. <https://doi.org/10.1021/acsami.6b11043>
25. Samyn, P. (2021). Polydopamine and Cellulose: Two Biomaterials with Excellent Compatibility and Applicability. *Polymer Reviews*, *0(0)*, 1–41. <https://doi.org/10.1080/15583724.2021.1896545>
26. Wang, Y., Dong, J., Jin, J., & Jia, Y.-G. (n.d.). Polyrotaxane Crosslinked Self-Healing Hydrogels for Switchable Bioadhesion. *Macromolecular Chemistry and Physics*, *n/a(n/a)*, 2000461. <https://doi.org/10.1002/macp.202000461>
27. Lei, J., Mayer, C., Freger, V., & Ulbricht, M. (2013). Synthesis and Characterization of Poly(ethylene glycol) Methacrylate Based Hydrogel Networks for Anti-Biofouling Applications. *Macromolecular Materials and Engineering*, *298(9)*, 967–980. <https://doi.org/10.1002/mame.201200297>
28. Fan, Z., Xu, Z., Niu, H., Sui, Y., Li, H., Ma, J., & Guan, J. (2019). Spatiotemporal delivery of basic fibroblast growth factor to directly and simultaneously attenuate cardiac fibrosis and promote cardiac tissue vascularization following myocardial infarction. *Journal of Controlled Release*, *311–312*, 233–244. <https://doi.org/10.1016/j.jconrel.2019.09.005>
29. Guan, Y., Niu, H., Dang, Y., Gao, N., & Guan, J. (2020). Photoluminescent oxygen-release microspheres to image the oxygen release process in vivo. *Acta Biomaterialia*, *115*, 333–342. <https://doi.org/10.1016/j.actbio.2020.08.031>

30. Niu, H., Li, C., Guan, Y., Dang, Y., Li, X., Fan, Z., Shen, J., Ma, L., & Guan, J. (2020). High oxygen preservation hydrogels to augment cell survival under hypoxic condition. *Acta Biomaterialia*, *105*, 56–67. <https://doi.org/10.1016/j.actbio.2020.01.017>
31. Niu, H., Li, X., Li, H., Fan, Z., Ma, J., & Guan, J. (2019). Thermosensitive, fast gelling, photoluminescent, highly flexible, and degradable hydrogels for stem cell delivery. *Acta Biomaterialia*, *83*, 96–108. <https://doi.org/10.1016/j.actbio.2018.10.038>
32. Oveissi, F., Naficy, S., Loan Le, T. Y., F. Fletcher, D., & Dehghani, F. (2019). Polypeptide-affined interpenetrating hydrogels with tunable physical and mechanical properties. *Biomaterials Science*, *7*(3), 926–937. <https://doi.org/10.1039/C8BM01182F>
33. Wang, F., Li, Z., Khan, M., Tamama, K., Kuppusamy, P., Wagner, W. R., Sen, C. K., & Guan, J. (2010). Injectable, rapid gelling and highly flexible hydrogel composites as growth factor and cell carriers. *Acta Biomaterialia*, *6*(6), 1978–1991. <https://doi.org/10.1016/j.actbio.2009.12.011>
34. Chen, J.-P., & Chiu, S.-H. (2000). A poly(N-isopropylacrylamide-co-N-acryloxysuccinimide-co-2-hydroxyethyl methacrylate) composite hydrogel membrane for urease immobilization to enhance urea hydrolysis rate by temperature swing☆. *Enzyme and Microbial Technology*, *26*(5), 359–367. [https://doi.org/10.1016/S0141-0229\(99\)00181-7](https://doi.org/10.1016/S0141-0229(99)00181-7)
35. Li, Z., Guo, X., Palmer, A. F., Das, H., & Guan, J. (2012). High-efficiency matrix modulus-induced cardiac differentiation of human mesenchymal stem cells inside a thermosensitive hydrogel. *Acta Biomaterialia*, *8*(10), 3586–3595. <https://doi.org/10.1016/j.actbio.2012.06.024>
36. Lau, K., Paus, R., Tiede, S., Day, P., & Bayat, A. (2009). Exploring the role of stem cells in cutaneous wound healing. *Experimental Dermatology*, *18*(11), 921–933. <https://doi.org/10.1111/j.1600-0625.2009.00942.x>

37. Lee, D. E., Ayoub, N., & Agrawal, D. K. (2016). Mesenchymal stem cells and cutaneous wound healing: Novel methods to increase cell delivery and therapeutic efficacy. *Stem Cell Research & Therapy*, 7(1), 37. <https://doi.org/10.1186/s13287-016-0303-6>
38. Maxson, S., Lopez, E. A., Yoo, D., Danilkovitch-Miagkova, A., & LeRoux, M. A. (2012). Concise Review: Role of Mesenchymal Stem Cells in Wound Repair. *STEM CELLS Translational Medicine*, 1(2), 142–149. <https://doi.org/10.5966/sctm.2011-0018>
39. Liang, Y., Zhao, X., Hu, T., Han, Y., & Guo, B. (2019). Mussel-inspired, antibacterial, conductive, antioxidant, injectable composite hydrogel wound dressing to promote the regeneration of infected skin. *Journal of Colloid and Interface Science*, 556, 514–528. <https://doi.org/10.1016/j.jcis.2019.08.083>
40. Chen, K., Wang, F., Liu, S., Wu, X., Xu, L., & Zhang, D. (2020). In situ reduction of silver nanoparticles by sodium alginate to obtain silver-loaded composite wound dressing with enhanced mechanical and antimicrobial property. *International Journal of Biological Macromolecules*, 148, 501–509. <https://doi.org/10.1016/j.ijbiomac.2020.01.156>
41. Lansdown, A. B. G. (2006). Silver in Health Care: Antimicrobial Effects and Safety in Use. *Biofunctional Textiles and the Skin*, 33, 17–34. <https://doi.org/10.1159/000093928>
42. Liu, Y., Ma, W., Liu, W., Li, C., Liu, Y., Jiang, X., & Tang, Z. (2011). Silver(i)–glutathione biocoordination polymer hydrogel: Effective antibacterial activity and improved cytocompatibility. *Journal of Materials Chemistry*, 21(48), 19214–19218. <https://doi.org/10.1039/C1JM13693C>
43. Xie, Y., Liao, X., Zhang, J., Yang, F., & Fan, Z. (2018). Novel chitosan hydrogels reinforced by silver nanoparticles with ultrahigh mechanical and high antibacterial properties for accelerating wound healing. *International Journal of Biological Macromolecules*, 119, 402–412. <https://doi.org/10.1016/j.ijbiomac.2018.07.060>
44. Shan, M., Gong, C., Li, B., & Wu, G. (2017). A pH, glucose, and dopamine triple-responsive, self-healable adhesive hydrogel formed by phenylborate–catechol

- complexation. *Polymer Chemistry*, 8(19), 2997–3005.
<https://doi.org/10.1039/C7PY00519A>
45. *Soft Condensed Matter*—Richard A.L. Jones—Oxford University Press. (n.d.). Retrieved April 10, 2021, from <https://global.oup.com/ukhe/product/soft-condensed-matter-9780198505891?cc=us&lang=en&>
46. Chan, J. K. C. (2014). The Wonderful Colors of the Hematoxylin–Eosin Stain in Diagnostic Surgical Pathology. *International Journal of Surgical Pathology*, 22(1), 12–32.
<https://doi.org/10.1177/1066896913517939>
47. Bilic-Curcic, I., Kalajzic, Z., Wang, L., & Rowe, D. W. (2005). Origins of endothelial and osteogenic cells in the subcutaneous collagen gel implant. *Bone*, 37(5), 678–687.
<https://doi.org/10.1016/j.bone.2005.06.009>